



Article

Continuously Updated Digital Elevation Models (CUDEMs) to Support Coastal Inundation Modeling

Christopher J. Amante ^{1,2,*} , Matthew Love ^{1,2}, Kelly Carignan ^{1,2} , Michael G. Sutherland ¹, Michael MacFerrin ^{1,2} and Elliot Lim ^{1,2}

¹ Cooperative Institute for Research in Environmental Sciences (CIRES), University of Colorado Boulder, Boulder, CO 80309, USA; matthew.love@colorado.edu (M.L.); kelly.carignan@colorado.edu (K.C.); michael.sutherland@colorado.edu (M.G.S.); michael.macferrin@colorado.edu (M.M.); limdj@colorado.edu (E.L.)

² National Centers for Environmental Information (NCEI), National Oceanic and Atmospheric Administration (NOAA), Boulder, CO 80305, USA

* Correspondence: christopher.amante@colorado.edu

Abstract: The National Oceanic and Atmospheric Administration (NOAA) National Centers for Environmental Information (NCEI) generates digital elevation models (DEMs) that range from the local to global scale. Collectively, these DEMs are essential to determining the timing and extent of coastal inundation and improving community preparedness, event forecasting, and warning systems. We initiated a comprehensive framework at NCEI, the Continuously Updated DEM (CUDEM) Program, with seamless bare-earth, topographic-bathymetric and bathymetric DEMs for the entire United States (U.S.) Atlantic and Gulf of Mexico Coasts, Hawaii, American Territories, and portions of the U.S. Pacific Coast. The CUDEMs are currently the highest-resolution, seamless depiction of the entire U.S. Atlantic and Gulf Coasts in the public domain; coastal topographic-bathymetric DEMs have a spatial resolution of 1/9th arc-second (~3 m) and offshore bathymetric DEMs coarsen to 1/3rd arc-second (~10 m). We independently validate the land portions of the CUDEMs with NASA's Advanced Topographic Laser Altimeter System (ATLAS) instrument on board the Ice, Cloud, and land Elevation Satellite-2 (ICESat-2) observatory and calculate a corresponding vertical mean bias error of 0.12 m \pm 0.75 m at one standard deviation, with an overall RMSE of 0.76 m. We generate the CUDEMs through a standardized process using free and open-source software (FOSS) and provide open-access to our code repository. The CUDEM framework consists of systematic tiled geographic extents, spatial resolutions, and horizontal and vertical datums to facilitate rapid updates of targeted areas with new data collections, especially post-storm and tsunami events. The CUDEM framework also enables the rapid incorporation of high-resolution data collections ingested into local-scale DEMs into NOAA NCEI's suite of regional and global DEMs. Future research efforts will focus on the generation of additional data products, such as spatially explicit vertical error estimations and morphologic change calculations, to enhance the utility and scientific benefits of the CUDEM Program.

Keywords: digital elevation model; topography; bathymetry; coastal; inundation



Citation: Amante, C.J.; Love, M.; Carignan, K.; Sutherland, M.G.; MacFerrin, M.; Lim, E. Continuously Updated Digital Elevation Models (CUDEMs) to Support Coastal Inundation Modeling. *Remote Sens.* **2023**, *15*, 1702. <https://doi.org/10.3390/rs15061702>

Academic Editors: Sara Innangi and Michele Innangi

Received: 20 January 2023

Revised: 7 March 2023

Accepted: 15 March 2023

Published: 22 March 2023



Copyright: © 2023 by the authors. Licensee MDPI, Basel, Switzerland. This article is an open access article distributed under the terms and conditions of the Creative Commons Attribution (CC BY) license (<https://creativecommons.org/licenses/by/4.0/>).

1. Introduction

Approximately 40 percent of the United States (U.S.) population lives in coastal counties prone to flooding [1]. The National Oceanic and Atmospheric Administration (NOAA) National Centers for Environmental Information (NCEI) generates digital elevation models (DEMs) to support the modeling of coastal inundation, e.g., [2–12]. Coastal DEMs are representations of the Earth's solid surface that extend across the coastal land–water interface [13–18]. NCEI scientists, in collaboration with the Cooperative Institute for Research in Environmental Sciences (CIRES) at the University of Colorado Boulder, generate coastal

DEMs by seamlessly integrating bathymetric and topographic datasets from numerous federal, state, and local government agencies [14,18–21]. Accurate, topographic-bathymetric DEMs are essential to coastal flood modeling as the shape and depth of the ocean floor affects the speed and height of waves [22–26], and the coastal land topography primarily determines the inland extent of inundation [21]. NOAA NCEI DEMs have spatial coverages that range from the local (e.g., [8]), to regional (e.g., [12]), to global scale (e.g., [2]), and, collectively, the suite of DEMs is used to model coastal inundation, e.g., [27–30].

1.1. Overview of NCEI DEMs

NOAA NCEI in Boulder, Colorado, formerly the National Geophysical Data Center (NGDC), developed the topographic-bathymetric global relief model, ETOPO5, in 1993, at a spatial resolution of 5 arc-minutes (~10 km) [31]. NGDC generated subsequent global relief models at finer spatial resolutions of 2 arc-minutes (~4 km) [32] and 1 arc-minute (~2 km) [2]. NGDC also generated regional coastal relief models (CRMs) of the U.S. Economic Exclusive Zone (EEZ) that extend to, and in certain locations beyond, the continental slope [12,33–42]. NGDC generated the first CRMs of the Northeast Atlantic [12] and Southeast Atlantic [33] in 1999, at a spatial resolution of 3 arc-seconds (~90 m) and the most recent CRM was updated in 2012, at a spatial resolution of 1 arc-second (~30 m) [41]. At the local scale, NGDC first developed a community-based DEM for Myrtle Beach, South Carolina, in 2006, at a spatial resolution of 1/3rd arc-second (~10 m) to support tsunami inundation modeling [43]. Between 2002 and 2014, NGDC generated more than one hundred DEMs for communities to support tsunami and storm surge inundation modeling efforts, hazard mitigation, and community preparedness, e.g., [4–7,9–11,44,45]. NGDC, in addition to the National Oceanic Data Center (NODC) and National Climatic Data Center (NCDC), were consolidated into NCEI in 2015. NCEI is responsible for hosting and providing access to one of the most significant environmental data archives on Earth, with comprehensive oceanic, atmospheric, and geophysical data.

1.2. DEM Projects

As CIRES scientists at NCEI, we generate local-scale DEMs to provide essential data for modeling coastal inundation for specific communities. These DEM development efforts have primarily been funded by the NOAA National Weather Service (NWS), NOAA Tsunami Program, and National Tsunami Hazard Mitigation Program (NTHMP). We initiated a comprehensive DEM development framework in collaboration with the U.S. Geological Survey (USGS) in 2014 to provide our modeling partners with coastal DEMs generated with consistent methodologies and specifications [46]. Since 2014, the framework has been enhanced to support coastal inundation modeling for the NOAA Tsunami Program, NTHMP, and the Consumer Option for an Alternative System to Allocate Losses (COASTAL) Act. More recently, we generated additional DEMs and advanced this framework with funding from the Bipartisan Budget Act of 2018: NOAA Supplemental Funding for Hurricanes Harvey, Irma, and Maria and through our support of the USGS as part of the National Oceanographic Partnership Program (NOPP) Predicting Hurricane Coastal Impacts, FY21–24 project.

1.2.1. NOAA Tsunami Program and National Tsunami Hazard Mitigation Program

The NOAA Tsunami Program, administered by the NWS, is an effort to minimize the impacts of tsunamis on coastal communities through effective, timely warnings and evacuations. The NOAA Tsunami program leverages the capabilities of the NWS and various NOAA line offices, including the Office of Oceanic and Atmospheric Research (OAR), National Ocean Service (NOS), and the National Environmental Satellite, Data, and Information Service (NESDIS). NCEI, as part of NESDIS, produces high-resolution coastal DEMs and is the long-term archive for national and international tsunami data, a natural hazards image database, and the global historical tsunami database.

NCEI DEMs are used for both the forecast (e.g., [47–50]) and the inundation mapping (e.g., [51–58]) components of the NOAA Tsunami Program and NTHMP. In the forecasting component, a precomputed scenario provides an estimate of wave arrival time, height, and inundation immediately after a tsunami triggering event. The numerical model incorporates a set of spatially nested DEMs, ranging from low-spatial resolution DEMs at the ocean basin scale to high-resolution at the coast, to resolve the changing wavelength as the tsunami moves into shallower waters [55]. The inundation modeling relies on high-resolution DEMs to provide information about the potential wave height, speed, and maximum inundation line at specific community locations. The development of inundation maps is fundamental to tsunami preparedness and planning efforts to understand and assess a communities' tsunami hazard. Tsunami propagation and inundation numerical models require the most current and accurate bathymetric and topographic data to reliably assess the potential impacts of tsunami events [50]. More up-to-date tsunami hazard assessments facilitate improved response plans and evacuation maps, and thereby, help save lives.

1.2.2. Consumer Option for an Alternative System to Allocate Losses (COASTAL) Act

The COASTAL Act was signed into law on 6 July 2012 [59]. The purpose of the COASTAL Act is to lower costs to the Federal Emergency Management Agency's (FEMA) National Flood Insurance Program (NFIP) by better determining wind versus water damage for "indeterminate losses" from damaging tropical cyclones in the U.S. and its territories. Indeterminate losses are where little tangible evidence beyond a building's foundation remains for insurance claim adjustments. The COASTAL Act requires NOAA to produce detailed "post-storm assessments" that contain outputs from a hindcast model indicating the strength and timing of damaging winds and water at specific building foundation locations. Results that are certified by NOAA as being greater than 90 percent accurate will then be input into a FEMA-managed formula to determine the appropriate loss allocation between wind and water damage.

We generate DEMs at NCEI for the COASTAL Act to support NOS storm surge modeling and, secondarily, the Office of Water Prediction (OWP) National Water Model (NWM) riverine modeling. NOS storm surge modelers use NCEI DEMs to update the Hurricane Surge On-demand Forecast System (HSOFS) unstructured grid for the Gulf of Mexico and Atlantic Ocean. The grid extends on land areas up to a topographic height of 10 m with a grid resolution of approximately 200 m, with finer spatial resolutions representing hydrologically important channels and topographic features. NCEI DEMs are improving the representation of these important topographic and bathymetric features in regions vulnerable to inundation and the refined HSOFS grid is being evaluated with the Advanced Circulation Model (ADCIRC)-WAVEWATCH III (WW3) coupled model system [60] to ensure numerical soundness and stability. NCEI DEMs are secondarily supporting the NWM, which is the foundation for riverine hydrologic forecasting. NWM provides river channel discharge within the continental United States (CONUS) including coastal zones, and ultimately, the NWM freshwater model will be coupled to the ocean models Extratropical Surge and Tide Operational Forecast System (ESTOFS) and ADCIRC [61].

1.2.3. Bipartisan Budget Act of 2018: NOAA Supplemental Funding for Hurricanes Harvey, Irma, and Maria

The Bipartisan Budget Act of 2018 was signed into law on February 9, 2018 [62]. NOAA NCEI received supplemental appropriations for disaster-related response and recovery efforts associated with Hurricanes Harvey, Irma, and Maria, with a focus on enhancing marine geophysical data management tools. This funding is supporting the ingest and archive of marine geophysical data collected in areas impacted by Hurricanes Irma, Harvey, and Maria, and the use of post-storm topographic-bathymetric lidar and multibeam swath bathymetric data to update NCEI's coastal DEMs in those areas. The funding is also supporting research on new methods to facilitate the rapid incorporation of updated DEMs

into regional and global elevation models, which will maximize the value of post-storm data and ensure scientific modeling efforts use elevation models that best reflect the current morphology across spatial scales.

1.2.4. National Oceanographic Partnership Program (NOPP) Predicting Hurricane Coastal Impacts, FY21-24

As part of the NOPP Predicting Hurricane Coastal Impacts, FY21-24 effort, the USGS is generating coastal DEMs and land surface variables for use in forecasting hurricane impacts. We are supporting USGS efforts on this project by generating high-resolution coastal DEMs to improve the accuracy of forecasting hurricane impacts including coastal wave, current, and sediment transport models used in the hindcast modeling of CONUS landing hurricanes. The USGS Earth Resources Observation and Science (EROS) Center generates coastal DEMs as part of their Coastal National Elevation Database (CoNED) Project [13,16]. NOAA NCEI and USGS EROS continue to collaboratively develop best-practices for DEM generation [46], although final DEM specifications, e.g., spatial extents and resolution, horizontal and vertical reference systems, can vary between NOAA NCEI and USGS EROS DEMs due to specific project requirements. We are currently collaborating with USGS EROS to generate new and updated coastal DEMs in hurricane-prone areas of the CONUS and to collate the best available coastal DEMs from NOAA NCEI and USGS EROS based on spatial resolution, vertical accuracy, and the date of generation.

1.3. Motivation for Comprehensive DEM Program

There were two primary motivations to initiate a comprehensive DEM program at NOAA NCEI. The first motivation was the need to rapidly and seamlessly update high-resolution, local-scale DEMs, especially in dynamic regions after morphological changes from currents, tides, storm surge, waves, and tsunamis. Between 2002 and 2014, NOAA NCEI was typically tasked to generate DEMs for individual coastal communities according to funders' specifications. Such project-based specifications included the DEM spatial resolution, spatial extents to include important features for community-based coastal modeling, horizontal reference (e.g., geographic or local projected coordinate systems), vertical reference (e.g., orthometric or tidal-based vertical datums), and raster storage registration (e.g., pixel- or grid-node registrations). We were often tasked to generate adjacent project-based DEMs years apart, and differences in the source datasets available at the time of the DEM generation exacerbated vertical offsets at the boundaries of DEMs caused by incongruent spatial resolutions, spatial extents and overlaps, horizontal datums, vertical datums, and raster registrations (Figure 1). Such DEM boundary condition differences can cause inaccurate and unstable coastal modeling results. Further, incongruent DEM specifications require additional processing steps to both update adjacent community DEMs with new topographic and bathymetric data collections and to ingest the resulting updated DEMs into regional and global elevation models.

The importance of nested local, regional, and global elevation models for coastal inundation modeling is the second motivation for a comprehensive DEM development program. Local, community-scale DEMs that integrate topography and bathymetry are essential for modeling waves and inundated coastal land areas. However, the speed and magnitude of tsunami wave propagation and inundation is affected by both near- and off-shore bathymetric features [22–26]. Similarly, storm surge and associated wave action are modeled at the basin scale (e.g., North Atlantic Ocean) on unstructured mesh grids with coarser resolutions in deeper waters and are imperative for warning systems providing forecasts days before the expected landfall. Inaccurate regional and global bathymetry models can cause coastal inundation modeling instability, particularly in areas offshore with large terrain slopes (e.g., Puerto Rico). In a comprehensive DEM development program, new data collections can be used to rapidly update local DEMs, which are then ingested into regional and global DEMs to minimize artificial elevation and depth discontinuities at the domain boundaries between nested spatial scales.

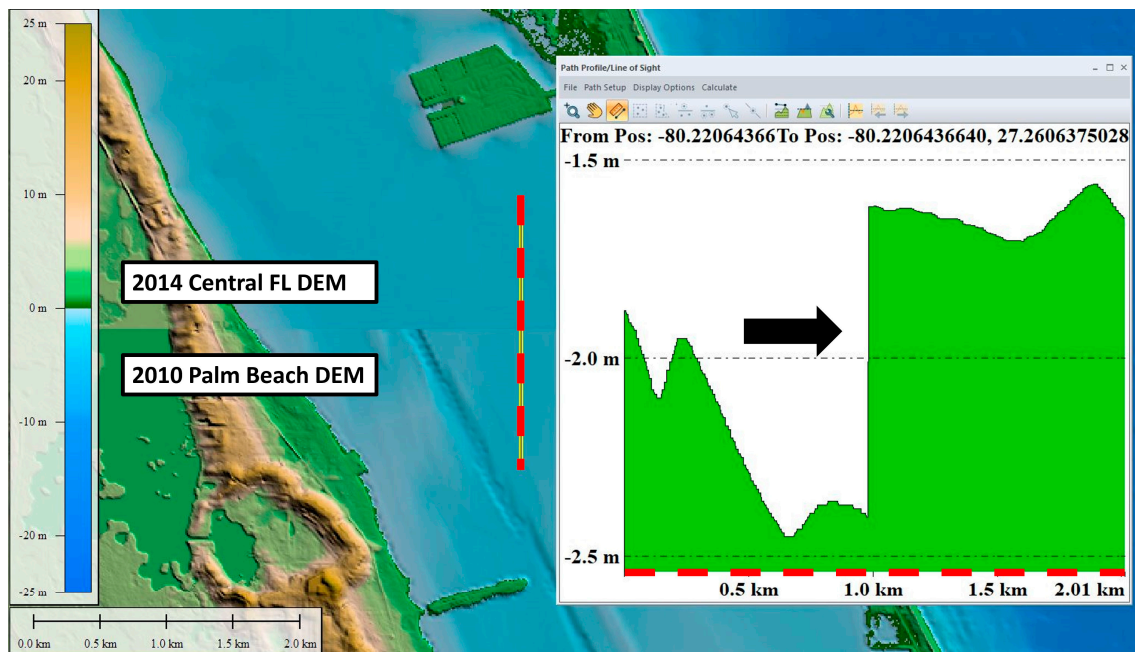


Figure 1. Differences in adjacent project-based DEM specifications and available source data at the time of generation can result in vertical offsets at the boundaries of DEMs. A topographic profile across the DEM boundary (red-dashed line) indicates a nearly 1 m offset (black arrow) in important coastal areas between the NOAA NCEI 2014 Central FL DEM and 2010 Palm Beach DEM.

The accuracy of local DEMs is continuously improving with modern topography and bathymetry data acquisition technologies. Modern aerial lidar and sonar data, as well as recent technical advances in structure from motion from multi-view stereo imagery with unmanned aerial vehicles (UAVs) [63,64] and the fusion of space-borne lidar and optical imagery [65], are continuously increasing the accuracy of representing present-day morphology in DEMs. Tsunamis, storm surge, and wave action can also cause morphological change, especially along dynamic, sandy coastlines [30,66–68], which necessitates continual updates to coastal DEMs. Post-event data collections should be used to rapidly update local DEMs, and at the same time, update regional and global elevation models. These two main factors provide the motivation for a comprehensive program to facilitate the systematic and efficient development and update of DEMs across all spatial scales. As members of the NOAA NCEI DEM Team through CIRES, the authors of this manuscript initiated a comprehensive program to develop a consistent, multi-resolution suite of tiled continuously updated DEMs, referred to hereafter as the “CUDEMs”, that rapidly incorporates the most modern topographic and bathymetric data at the local, regional, and global scale.

2. Materials and Methods

2.1. Study Area

We generated CUDEM tiles for the entire U.S. Atlantic and Gulf of Mexico Coasts, Hawaii, Puerto Rico, U.S. Virgin Islands (USVI), American Samoa, Guam, and the Commonwealth of the Northern Mariana Islands (CNMI) to support coastal inundation modeling (Figure 2). We generated the integrated topographic-bathymetric DEMs at a spatial resolution of 1/9th arc-second (~3 m) and additional offshore bathymetric DEMs at a coarser resolution of 1/3rd arc-second (~10 m) to support storm surge and wave modeling for the COASTAL Act. The coastal DEMs extend inland to the NOAA National Hurricane Center (NHC) Maximum of the Maximum envelope of high water (MOM). The MOM extent provides a worst-case snapshot for a particular storm category under combinations of forward speed, trajectory, and initial tide level for hurricane evacuation planning and to develop the nation’s evacuation zones [69]. We generated DEMs for the COASTAL Act

to the MOM inland extent for a Category 4 hurricane for Virginia, U.S. northward and Category 5 hurricane south of Virginia. The MOM inland extent and resulting CUDEM coverage is primarily determined by coastal elevations and terrain slope. The elevation-based nature ensures that CUDEMs are available for modeling inland impacts from extreme storms, especially for low-lying, flat coastal areas such as the U.S. southeastern Atlantic and Gulf Coast. The NOAA Tsunami Program and NTHMP funded NCEI DEM development for portions of the U.S. Pacific Coast, including Alaska, Washington State, Oregon, and California as specified by modelers. NCEI Pacific Coast DEMs generated for NTHMP extend inland to the tsunami inundation line determined by state inundation modelers and also include additional bathymetric DEMs offshore for modeling the tsunami wavelength as it travels into coastal waters.

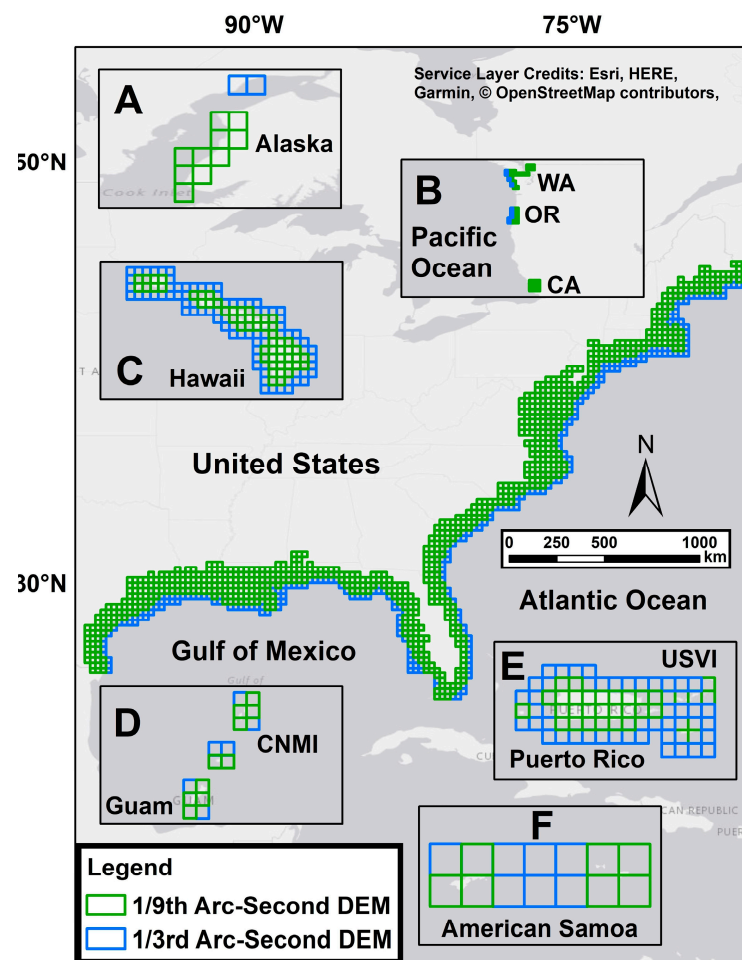


Figure 2. NOAA NCEI-tiled CUDEM footprints as of October 2022. The CUDEMs cover the entire U.S. Atlantic and Gulf of Mexico Coasts, and the lettered inserts show the portions of (A) Alaska and (B) Washington (WA), Oregon (OR) and California (CA) Coasts, and the entirety of (C) Hawaii, (D) Guam and CNMI, (E) Puerto Rico and USVI, and (F) American Samoa.

2.2. Continuously Updated DEM Program

The concept of a comprehensive DEM Program at NOAA NCEI originated in 2014 with the development of systematic tiled DEMs with Post-Hurricane Sandy topographic and bathymetric data collections. NOAA NCEI and the USGS jointly determined DEM specifications to model coastal land elevations and water depths for the coastal areas impacted by Hurricane Sandy as part of a broader framework to seamlessly depict merged topography and bathymetry along U.S. coasts [46]. We initiated the CUDEM Program to facilitate the rapid update of NCEI DEMs with new bathymetric and topographic data

collections and to improve consistency across NCEI's suite of local, regional, and global DEMs. The CUDEM Program includes DEM generation in a geographic coordinate system (i.e., North American Datum of 1983), the official National Geodetic Survey (NGS) vertical datums for the CONUS, Hawaii, and U.S. Island Territories (Table 1), pixel-node (area) raster registration [70], and systematic 0.25 decimal degree tile extents (~25 km by 25 km).

Table 1. Vertical datum specifications for the CUDEMs. ** Note that there is no unified vertical reference for Hawaii, and we generated the DEMs relative to approximately local mean sea level. See Cooper [71] and references therein for additional information on vertically referencing elevation data in Hawaii.

Geographic Location	Vertical Datum	Dates
CONUS	North American Vertical Datum of 1988 (NAVD88)	1992–present
Hawaii	** Local Mean Sea Level	–
Puerto Rico	Puerto Rico Vertical Datum of 2002 (PRVD02)	2002–present
USVI	Virgin Islands Vertical Datum of 2009 (VIVD09)	2009–present
Guam	Guam Vertical Datum of 2004 (GUVVD04)	2004–present
CNMI	Northern Marianas Vertical Datum of 2003 (NMVD03)	2003–present
American Samoa	American Samoa Vertical Datum of 2002 (ASVD02)	2002–2020

We generate the CUDEMs at a spatial resolution of 1/9th arc-second along the coastline where we integrate topographic and bathymetric datasets and 1/3rd arc-second farther offshore where there are typically sparser bathymetric source data. The spatial resolutions reflect the typical elevation measurement data density in many U.S. coastal areas: dense, topographic and bathymetric lidar measurements nearshore, and sparse, legacy sonar and lead line measurements offshore, especially in shallow, continental shelves [46]. The vertical units for all CUDEMs are meters and the raster file format is Georeferenced Tiff (Geotiff).

In addition to consistent DEM horizontal and vertical reference systems and spatial resolutions, the 0.25 decimal degree tile extents framework facilitates rapid updates of targeted areas with new data collections, especially post-storm and tsunami events. The tiled framework enabled the rapid update of CUDEMs with post-Hurricane Harvey (Texas) and Maria (Puerto Rico and USVI) topographic and bathymetric lidar and sonar data collections as part of the Bipartisan Budget Act of 2018: NOAA Supplemental Funding for Hurricanes Harvey, Irma, and Maria [62]. At the time of publication, we are currently ingesting post-Hurricane Irma topographic and bathymetric lidar and sonar data collections to update CUDEMs in southwest Florida. As part of this project, we conducted research to rapidly incorporate updated local DEMs into regional and global elevation models, which will maximize the value of post-storm data and ensure scientific modeling efforts utilize elevation models that best reflect the current morphology across spatial scales. Specifically, additional bathymetric DEM tiles offshore Puerto Rico were generated at 1 arc-second (~30 m) and merged with 1/9th arc-second and 1/3rd arc-second tiles to create a regional CRM of Puerto Rico at 1 arc-second spatial resolution. We are also developing additional CRMs at the regional scale along the U.S. Atlantic and Gulf Coasts. Most recently, we generated a new, global relief model, ETOPO 2022, at 15 arc-second (~0.5 km) spatial resolution in the CUDEM framework that incorporated all of the higher resolution CUDEMs [72].

2.3. DEM Generation with Free and Open Source Software

We generate the CUDEMs through a standardized process using free and open-source software (FOSS) and provide open-access to our code repository for consistency, trans-

parency, and to promote accessibility [73]. DEM development at NOAA NCEI is an iterative process with multiple quality-control (QC) measures. The general DEM development workflow (Figure 3) consists of:

1. Gather elevation data;
2. Convert data to common vertical and horizontal datums, units, and file formats;
3. Evaluate and edit data in GIS software;
4. Build and evaluate DEMs in GIS software and with statistical analyses;
5. Document DEM development in technical reports and metadata;
6. Distribute DEMs for public availability.

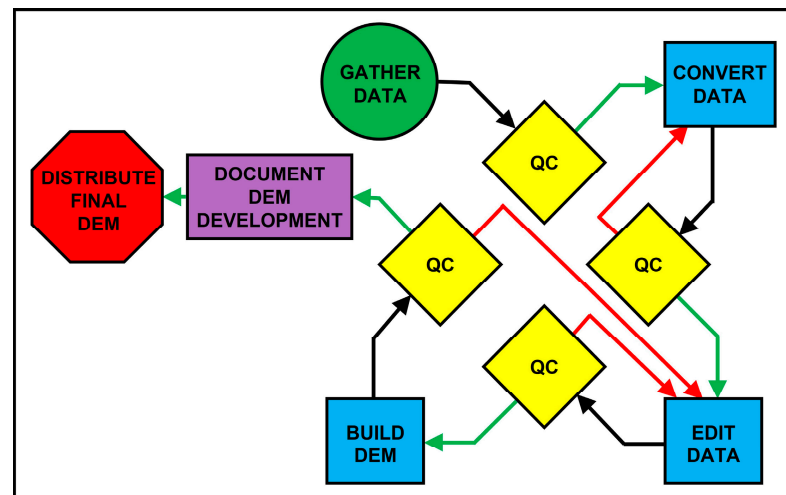


Figure 3. The DEM development workflow at NOAA NCEI is an iterative process of gathering elevation and depth data from multiple sources, converting the data to common specifications, and editing the data prior to building the DEM. There are multiple, iterative quality-control (QC) measures in the workflow, and we document the DEM development process prior to the final DEM distribution.

Specifically, the open-access code includes command-line tools and a Python application programming interface (API) for automated data download, processing, QC, gridding, and formatting with two main software tools: “fetches” and “waffles.” “Fetches” is the data download tool for obtaining publicly available elevation data from a variety of sources and can optionally list, download or process the fetched data for use in DEM generation. We download a variety of data types, e.g., topographic lidar, multibeam swath sonar bathymetry, hydrographic soundings, etc., from a variety of sources, e.g., NOAA Office for Coastal Management (OCM) Digital Coast, NOAA NCEI NOS Hydrographic Surveys, NOAA NCEI Multibeam, USGS The National Map, and U.S. Army Corps of Engineers (USACE) Navigation Condition Surveys, etc. (Table 2). Data from these sources are collected by different instruments, on different platforms, and in different environments. Other data sources include digitized bathymetric charts or topographic maps, shorelines, satellite-derived elevations, and precisely surveyed geodetic monuments. We download the data in an area slightly larger (~5%) than the DEM extents. This data “buffer” ensures that interpolative gridding occurs across rather than along the DEM boundaries to prevent edge effects, which is especially important in areas with sparse bathymetric data and large interpolation distances. Data buffers also minimize vertical offsets between adjacent DEM tiles. We use MB-System [74] style datalists to evaluate and process the large amount of varied source elevation data, including fetching data on-the-fly using any of the available “fetches” data modules listed in Table 2.

Table 2. Data source modules available in the CUDEM software tool “fetches.”

Name	Description	URL
Arcticdem	Arctic DEM	https://www.pgc.umn.edu/data/arcticdem/
Bluetopo	A curated collection of high- resolution seafloor models from NOAA.	https://www.nauticalcharts.noaa.gov/data/bluetopo.html
Buoys	Buoy information from NOAA	https://www.ndbc.noaa.gov
Charts	NOS Nautical Charts, including electronic Nautical Charts and Raster Nautical Charts	https://www.charts.noaa.gov/
Chs	Canadian Hydrographic Surveys	https://open.canada.ca
copernicus	Copernicus elevation data	https://doi.org/10.5069/G9028PQB
digital_coast	Lidar and Raster data from NOAA’s Digital Coast	https://coast.noaa.gov
Earthdata	NASA Earthdata	https://cmr.earthdata.nasa.gov
Ehydro	USACE hydrographic surveys	https://navigation.usace.army.mil/Survey/Hydro
Emodnet	EmodNET European Bathymetric/Topographic DEM	https://portal.emodnet-bathymetry.eu/
Fabdem	FABDEM (Forest and Buildings removed Copernicus DEM)	https://data.bris.ac.uk/data/dataset/s5hqmjcdj8yo2ibzi9b4ew3sn
Gebco	A global continuous terrain model for ocean and land with a spatial resolution of 15 arc-seconds.	https://www.gebco.net/data_and_products/gridded_bathymetry_data/
Gmrt	The Global MultiResolution Topography synthesis	https://www.gmrt.org
Hrdem	High-Resolution DEMs from Canada	https://open.canada.ca
hydrolakes	HydroLakes vector and derived elevations	https://www.hydrosheds.org/products/hydrolakes
mar_grav	Marine Gravity Satellite Altimetry Topography from Scripps.	https://topex.ucsd.edu/WWW_html/mar_grav.html
Mgds	Marine Geoscience Data System	https://www.marine-geo.org
Multibeam	NOAA Multibeam bathymetric data	https://data.ngdc.noaa.gov/platforms/
Nasadem	NASA Digital Elevation Model	https://www.earthdata.nasa.gov/esds/competitive-programs/measures/nasadem
neci_thredds	NCEI DEM THREDDS Catalog	https://www.ngdc.noaa.gov/thredds/catalog/demCatalog.html
Ngs	NGS monuments	http://geodesy.noaa.gov/
Nos	NOS Hydrographic DataBase (NOSHDB)	https://www.ngdc.noaa.gov/mgg/bathymetry/hydro.html
Osm	Open Street Map	https://wiki.openstreetmap.org/
srtm_plus	SRTM15+: Global bathymetry and topography at 15 arc-seconds.	https://topex.ucsd.edu/WWW_html/srtm15_plus.html
Tides	Tide station information from NOAA	https://tidesandcurrents.noaa.gov/
Tnm	USGS National Map	https://apps.nationalmap.gov/tnmaccess/
Trackline	NOAA trackline bathymetry data	http://www.ngdc.noaa.gov/trackline/
Usiei	US Interagency Elevation Inventory	https://coast.noaa.gov/inventory/
Vdatum	Vertical Datum transformation grids	https://vdatum.noaa.gov ; https://cdn.proj.org/

All URL are accessed on 14 March 2023.

We visualize each data source in various GIS software applications, including Global Mapper, QGIS, and ArcGIS. A visual assessment of a data source may reveal gross discrepancies between adjacent elevation or depth measurements caused by several factors such as misclassification of feature types (e.g., tree canopy or bare-earth), sound velocity errors, or incorrect digitization. Where multiple datasets overlap, there may be gross discrepancies between data sources due to disparate spatial resolutions, age, and instrumentation. In these areas of overlap, we visually compare and quantify the accuracy of each dataset with independent measurements, consider the data collection date, and then typically remove the less accurate, older data to reduce artifacts in the final DEMs. In areas of sparse or no data where there are known to be features such as rocks, jetties, etc., manual digitization may be required to incorporate these features into the final DEM. Additional

data processing steps may include removing buildings and vegetation from misclassified lidar datasets, converting data into common units of measurement, or changing a depth measurement value sign from positive depths down to negative values referenced to a vertical datum [14].

Importantly, we process bathymetric and topographic data into common data formats, horizontal datums, and vertical datums to generate integrated, seamless coastal DEMs. Bathymetric data are typically referenced to a tidal datum (e.g., mean-lower-low water; MLLW) whereas topographic data are typically referenced to an orthometric datum (e.g., North American Vertical Datum of 1988; NAVD88), respectively. To ensure seamlessness across coastal areas, we convert the bathymetric data from their tidal datum into the orthometric datum of the topographic data (see Table 1). The other main CUDEM tool “waffles” includes numerous gridding modules for DEM development (Table 3). The “waffles” module “vdatum” generates a raster that represents a spatially varying relationship between a tidal datum and an orthometric datum based on the vertical datum transformation grids in NOAA’s VDatum Tool [75]. In cases where VDatum transformation grids are unavailable for a given region, the CUDEM “waffles” module “vdatum” generates a grid of the relationship between vertical datums using data from the nearest NOAA tidal stations.

Table 3. Gridding modules available in the CUDEM software tool “waffles.”

Name	Description
average	Generate an average DEM using GDAL’s <i>gdal_grid</i> command.
coastline	Generate a coastline (land/sea mask) using a variety of data sources.
cudem	CUDEM integrated DEM generation. Generate a topographic-bathymetric integrated DEM using a variety of data sources.
IDW	Generate a DEM using an Inverse Distance Weighted algorithm. If weights are used, will generate a UIDW DEM, using weight values as inverse uncertainty, as described here: https://ir.library.oregonstate.edu/concern/graduate_projects/79407x932 (accessed on 14 March 2023), and here: https://stackoverflow.com/questions/3104781/inverse-distance-weighted-idw-interpolation-with-python (accessed on 14 March 2023)
invdst	Generate an inverse distance DEM using GDAL’s <i>gdal_grid</i> command.
linear	Generate a linear DEM using GDAL’s <i>gdal_grid</i> command.
mbgrid	Generate a DEM using MB-System’s <i>mbgrid</i> command (spline interpolation).
nearest	Generate a nearest DEM using GDAL’s <i>gdal_grid</i> command.
nearneighbor	Generate a DEM using GMT’s <i>nearneighbor</i> command.
num	Generate an un-interpolated DEM using various gridding modes, including options from GMT’s <i>xyz2grd</i> command.
scipy	Generate a DEM using Scipy’s gridding algorithms (linear, cubic, nearest).
stacks	Generate a DEM using a raster stacking method. By default, calculate the (weighted) mean where overlapping cells occur. Set <i>supersede</i> to True to overwrite overlapping cells with higher weighted data.
surface	Generate a DEM using GMT’s <i>surface</i> command (spline interpolation).
triangulate	Generate a DEM using GMT’s <i>triangulate</i> command.
vdatum	Generate a vertical datum conversion grid.

Another important processing step, especially in coastal areas with dense topographic data and sparse bathymetric data, is the generation of a bathymetric surface. First, we generate a raster and vector coastline within a specified area based on Copernicus DEM [76] elevation values above and below mean sea level with the CUDEM “waffles” module “coastline.”. Additionally, the “coastline” module enables the incorporation of higher-resolution datasets to refine the resulting coastline. In areas where bathymetric and/or topographic lidar datasets are available, these data can be incorporated into the tool to

generate a coastline based on the input lidar data that are typically referenced to the same vertical datum as the final DEM. Next, we generate a bathymetric surface at a coarser resolution than the final DEM to interpolate bathymetric values in areas where there are sparse or no bathymetric data. The bathymetric surface reduces data artifacts often found within sparse bathymetric datasets and also improves interpolation into the coastal zone. Interpolating only the bathymetric values prevents dense, topographic data from interpolating across features such as river channels and coastal marshes, which would cause such areas in the DEMs to have inaccurate, higher elevation values. We then resample the resulting bathymetric surface to the resolution of the final DEM, mask the resampled raster to the generated coastline, and incorporate the masked raster as a dataset in the final DEM generation.

We generate the bathymetric surface, as well as the final DEM, with the various interpolative gridding modules within the CUDEM “waffles” tool (Table 3). Previous research at NCEI indicates spline interpolation is the most accurate gridding method for generating DEMs [20]. The CUDEM “waffles” tool applies gridding algorithms, such as the “surface” module, to generate the raster DEM using spline interpolation. Within the generated datalist, we specify the gridding weight to adjust the relative influence of the dataset to the DEM value. The gridding weight is determined based on our accuracy assessments, with larger values representing more accurate datasets and having greater influence on the DEM value in areas with overlapping or adjacent datasets. We typically apply a low-pass frequency filter, i.e., a fast Fourier transform (FFT)-based convolution with a Gaussian kernel [77], to reduce noise in the final DEM. There is also an optional user-provided parameter in the CUDEM command “waffles” to apply the filter below a specified elevation value. We typically only apply the filter in bathymetric areas of DEMs that are derived from sparse, inaccurate depth soundings to reduce interpolation artifacts in these areas. The CUDEM software tools and modules therein are all publicly available, free to use and modify, and can be accessed from the GitHub repository [73].

We QC and iteratively re-grid the DEMs until gross anomalies are resolved. Visual QC techniques include raster hillshades, 3-dimensional (3D) perspective views, and elevation value color shading to assist in identifying anomalies and artifacts in each iteration of the DEM. We also generate derivative products such as terrain slope and curvature rasters to help identify areas of artificial slopes and vertical discontinuities along the boundaries of datasets.

Lastly, CUDEM tiles are named in the following manner:

ncei[RR]_[n][YY]x[yy]_[W][XXX]x[xx]_[DDDD]v[#].tif

with the following information in place of the brackets []:

[RR]—“19” or “13”, for DEM tile resolution of 1/9th or 1/3rd in arc-seconds;

[n]—“n” or “s”, for Northern or Southern hemisphere;

[YY]x[yy]—Numeric latitude of tile’s northern (top) border in decimal degrees;

[W]—“W” or “E”, for Western or Eastern hemisphere;

[XXX]x[xx]—Numeric longitude of tile’s western (left) border in decimal degrees;

[DDDD]—Year of tile generation;

[#]—Version number of the release.

For example, a CUDEM tile named “ncei19_n39x00_w075x25_2014v1.tif” is a 1/9th arc-second resolution GeoTiff file with an upper-left corner at North 39.00 degrees latitude and West 75.25 degrees longitude, generated in the year 2014 and is the first version in this geographic space and resolution. As we continue to update CUDEMs, the year of generation and the version number for a specific geographic tile will be updated. Such standardization will facilitate direct comparison between the DEMs, quantitative change analysis, and assessments on improvements to the DEMs where new data sources were incorporated.

2.4. Spatial Metadata Generation

We started generating spatial metadata in 2019 to provide additional information on the source data used in the DEM development. The spatial metadata are generated

at a raster spatial resolution of 1/3rd arc-second for all CUDEMs and then vectorized to shapefile format to easily view numerous field attributes for each data source in a GIS software. The detailed shapefile polygons provide important information on the locations of the source elevation measurements from which the DEM values are derived.

2.5. Vertical Accuracy Assessment

We independently validated the land portions of the CUDEMs with NASA’s Advanced Topographic Laser Altimeter System (ATLAS) instrument on board the Ice, Cloud, and land Elevation Satellite-2 (ICESat-2) observatory. We used ICESat-2 to perform vertical accuracy assessments for individual CUDEM tiles and to determine the overall accuracy for the entire CUDEM collection. We converted the DEMs to a common vertical reference system (EGM2008) using the CUDEM “waffles” module “vdatum” for direct comparison with ICESat-2 ATL03/ATL08 [78,79] ground photons. We masked the DEMs to omit areas covered by ocean, inland lakes and reservoirs defined by the global HydroLakes dataset [80] and buildings defined by the global OpenStreetMap API [81] to restrict the vertical accuracy assessment to only ground elevations. We extracted the ICESat-2 photons from all satellite overpasses during the calendar year 2021, and then individually classified them as ground, vegetation canopy, or atmosphere/noise returns. We used only the ground-based photons for the accuracy assessment. To reduce potential noise, we performed accuracy assessments on DEM cells if the interdecile range (10–90%) of ICESat-2 ground photons within a DEM grid cell included at least 3 photons. The CUDEM vertical errors were then calculated as the differences between the DEM grid cell values and the mean elevations of the ICESat-2 ground photons within the same grid cells.

3. Results

3.1. CUDEMs

The CUDEMs are a shift from individual project-based DEM specifications to a comprehensive program that systematically and continuously generates new and updated DEMs across all spatial scales. We generated 925 1/9th arc-second DEMs and 403 1/3rd arc-second DEMs in the CUDEM framework between 2014 and 2022 (Table 4). These 1328 CUDEM tiles cover approximately 850,000 km² of U.S. coastal areas.

Table 4. The total number of NCEI CUDEM tiles generated to date.

CUDEM Subset Location: Vertical Datum	1/9th Arc-Second Tile Count	1/3rd Arc-Second Tile Count
CONUS: NAVD88	819	267
Hawaii: MSL	54	79
Puerto Rico: PRVD02	26	29
USVI: VIVD09	9	15
Guam: GUV04	4	2
CNMI: NMVD03	6	4
American Samoa: ASVD02	7	7
Total	925	403

3.2. Data Discovery and Access

The 1/9th and 1/3rd arc-second CUDEMs are discoverable and accessible for public download through the NOAA OCM Digital Coast Data Access Viewer (DAV; Table 5). The CUDEMs can also be downloaded for each spatial resolution via their respective bulk download pages.

Table 5. CUDEM data download URLs from the NOAA Digital Coast Data Access Viewer (DAV) and their respective bulk download pages.

CUDEM Subset Location: Vertical Datum	Data Access Viewer URL	Digital Coast Bulk Download URL
CUDEM 1/9th CONUS: NAVD88	https://coast.noaa.gov/dataviewer/#/lidar/search/where:ID=8483	https://chs.coast.noaa.gov/htdata/raster2/elevation/NCEI_ninth_Topobathy_2014_8483/
CUDEM 1/9th Hawaii: MSL	https://coast.noaa.gov/dataviewer/#/lidar/search/where:ID=9428	https://chs.coast.noaa.gov/htdata/raster2/elevation/NCEI_ninth_Topobathy_Hawaii_9428/
CUDEM 1/9th Puerto Rico: PRVD02	https://coast.noaa.gov/dataviewer/#/lidar/search/where:ID=9525	https://chs.coast.noaa.gov/htdata/raster5/elevation/NCEI_ninth_Topobathy_PuertoRico_9525/
CUDEM 1/9th USVI: VIVD09	https://coast.noaa.gov/dataviewer/#/lidar/search/where:ID=9529	https://chs.coast.noaa.gov/htdata/raster5/elevation/NCEI_ninth_Topobathy_USVI_9529/
CUDEM 1/9th Guam: GUV04	https://coast.noaa.gov/dataviewer/#/lidar/search/where:ID=9462	https://chs.coast.noaa.gov/htdata/raster5/elevation/NCEI_ninth_Topobathy_Guam_9462/
CUDEM 1/9th CNMI: NMVD03	https://coast.noaa.gov/dataviewer/#/lidar/search/where:ID=9560	https://chs.coast.noaa.gov/htdata/raster5/elevation/NCEI_ninth_Topobathy_CNMI_9560/
CUDEM 1/9th American Samoa: ASVD02	https://coast.noaa.gov/dataviewer/#/lidar/search/where:ID=9460	https://chs.coast.noaa.gov/htdata/raster5/elevation/NCEI_ninth_Topobathy_AmSam_9460/
CUDEM 1/3rd CONUS: NAVD88	https://coast.noaa.gov/dataviewer/#/lidar/search/where:ID=8580	https://chs.coast.noaa.gov/htdata/raster2/elevation/NCEI_third_Topobathy_2014_8580/
CUDEM 1/3rd Hawaii: MSL	https://coast.noaa.gov/dataviewer/#/lidar/search/where:ID=9429	https://chs.coast.noaa.gov/htdata/raster2/elevation/NCEI_third_Topobathy_Hawaii_9429/
CUDEM 1/3rd Puerto Rico: PRVD02	https://coast.noaa.gov/dataviewer/#/lidar/search/where:ID=9524	https://chs.coast.noaa.gov/htdata/raster5/elevation/NCEI_third_Topobathy_PuertoRico_9524/
CUDEM 1/3rd USVI: VIVD09	https://coast.noaa.gov/dataviewer/#/lidar/search/where:ID=9528	https://chs.coast.noaa.gov/htdata/raster5/elevation/NCEI_third_Topobathy_USVI_9528/
CUDEM 1/3rd Guam: GUV04	https://coast.noaa.gov/dataviewer/#/lidar/search/where:ID=9463	https://chs.coast.noaa.gov/htdata/raster5/elevation/NCEI_third_Topobathy_Guam_9463/
CUDEM 1/3rd CNMI: NMVD03	https://coast.noaa.gov/dataviewer/#/lidar/search/where:ID=9561	https://chs.coast.noaa.gov/htdata/raster5/elevation/NCEI_third_Topobathy_CNMI_9561/
CUDEM 1/3rd American Samoa: ASVD02	https://coast.noaa.gov/dataviewer/#/lidar/search/where:ID=9461	https://chs.coast.noaa.gov/htdata/raster5/elevation/NCEI_third_Topobathy_AmSam_9461/

All URL are accessed on 14 March 2023.

3.3. Documentation

We generated documentation on the CUDEM specifications, input data sources, processing, and gridding for regional project areas [82]. We also generated Federal Geographic Data Committee (FGDC) compliant and International Organization for Standardization (ISO) 19115-2 standard metadata (Table 6). The metadata records contain the elements to meet NCEI requirements and provide valuable information to assist users, such as the

spatial representation and reference system information. Published metadata records are then harvested and ingested into publicly searchable data catalogs.

Table 6. DOI and metadata records for the CUDEM collections, separated by spatial resolution and vertical datum.

Top Level CUDEM Record DOI	CUDEM Subset Location: Vertical Datum	Metadata Record URL
CUDEM 1/9th arc-second; https://doi.org/10.25921/ds9v-ky35	–	https://data.noaa.gov/waf/NOAA/NESDIS/NGDC/MGG/DEM/iso/xml/999919.xml
	CONUS: NAVD88	https://data.noaa.gov/waf/NOAA/NESDIS/NGDC/MGG/DEM/iso/xml/199919.xml
	Hawaii: MSL	https://data.noaa.gov/waf/NOAA/NESDIS/NGDC/MGG/DEM/iso/xml/299919.xml
	Puerto Rico: PRVD02	https://data.noaa.gov/waf/NOAA/NESDIS/NGDC/MGG/DEM/iso/xml/399919.xml
	USVI: VIVD09	https://data.noaa.gov/waf/NOAA/NESDIS/NGDC/MGG/DEM/iso/xml/499919.xml
	Guam: GUV04	https://data.noaa.gov/waf/NOAA/NESDIS/NGDC/MGG/DEM/iso/xml/599919.xml
	CNMI: NMVD03	https://data.noaa.gov/waf/NOAA/NESDIS/NGDC/MGG/DEM/iso/xml/699919.xml
	American Samoa: ASVD02	https://data.noaa.gov/waf/NOAA/NESDIS/NGDC/MGG/DEM/iso/xml/799919.xml
CUDEM 1/3rd arc-second; https://doi.org/10.25921/0mpp-h192	–	https://data.noaa.gov/waf/NOAA/NESDIS/NGDC/MGG/DEM/iso/xml/999913.xml
	CONUS: NAVD88	https://data.noaa.gov/waf/NOAA/NESDIS/NGDC/MGG/DEM/iso/xml/199913.xml
	Hawaii: MSL	https://data.noaa.gov/waf/NOAA/NESDIS/NGDC/MGG/DEM/iso/xml/299913.xml
	Puerto Rico: PRVD02	https://data.noaa.gov/waf/NOAA/NESDIS/NGDC/MGG/DEM/iso/xml/399913.xml
	USVI: VIVD09	https://data.noaa.gov/waf/NOAA/NESDIS/NGDC/MGG/DEM/iso/xml/499913.xml
	Guam: GUV04	https://data.noaa.gov/waf/NOAA/NESDIS/NGDC/MGG/DEM/iso/xml/599913.xml
	CNMI: NMVD03	https://data.noaa.gov/waf/NOAA/NESDIS/NGDC/MGG/DEM/iso/xml/699913.xml
	American Samoa: ASVD02	https://data.noaa.gov/waf/NOAA/NESDIS/NGDC/MGG/DEM/iso/xml/799913.xml

All URL are accessed on 14 March 2023.

3.4. Spatial Metadata

The FGDC compliant metadata and spatial metadata products are available for download for each spatial resolution and vertical datum from their respective bulk download pages (see Table 5). We started generating spatial metadata for CUDEMs in 2019, and to date, includes coverage of the Gulf of Mexico, New England, Hawaii, Puerto Rico, American Samoa, Guam, and portions of the U.S. West Coast. The spatial metadata enhance standard text-based metadata by indicating the locations of the source datasets used in the development of the DEMs and provide valuable information including the data collection agency and the year of collection (Figure 4). Previous research at NCEI indicates that the vertical uncertainty in DEMs varies spatially due to the integration of disparate data collected at different time periods and with different measurement technologies (e.g.,

sonar, lidar) [18]. The spatial component can help users infer the relative accuracy of areas within the DEM based on the age, density, and instrumentation of the underlying data. For example, the accuracy of the DEM typically decreases in areas with old, sparse, lead line measurements with large interpolation distances [18–20]. The spatial metadata also enable source data provenance and can facilitate data masking for future DEM updates with new data collections. For example, the spatial metadata shapefile can be used to remove areas of the DEM derived from pre-storm data where there are new, post-storm data collections to update the DEM.

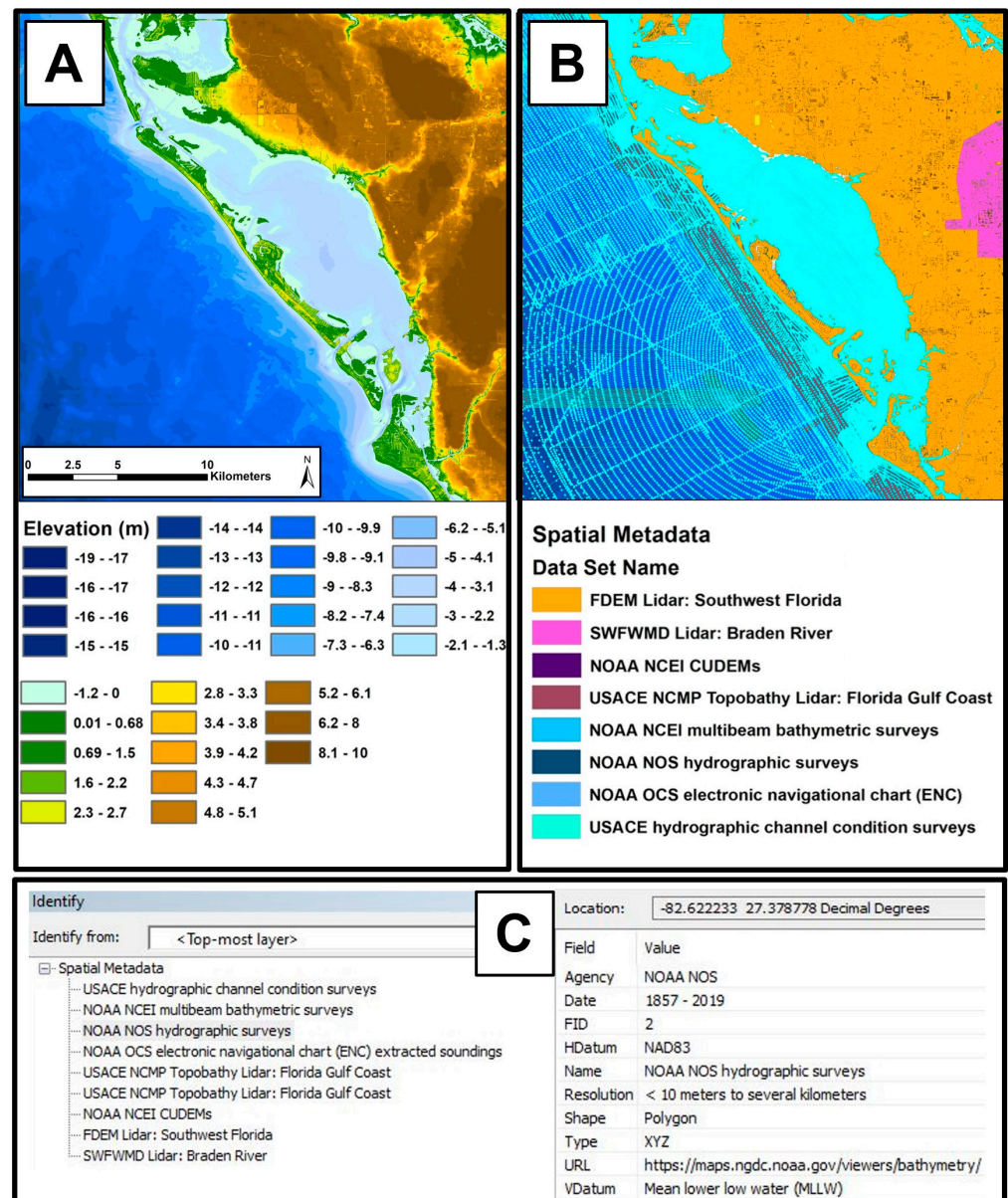


Figure 4. An example of the CUDEM spatial metadata shapefile product: (A) CUDEM tile “ncei19_n27X50_w082X75_2020v1.tif” elevation values, (B) highlighted data source “NOAA NOS hydrographic surveys” shows the location of the individual measurements and indicate sparser measurements offshore, (C) attribute table of highlighted data source includes valuable information such as the data collection agency and the year of collection.

3.5. Vertical Accuracy

We independently validated the land portions of the 1/9th arc-second CUDEMs with NASA’s ATLAS instrument on board the ICESat-2 observatory and calculated a

corresponding vertical mean bias error of $0.12 \text{ m} \pm 0.75 \text{ m}$ at one standard deviation, with an overall RMSE of 0.76 m (Figure 5, Panel A). See Table 7 for the vertical accuracy statistics of the CUDEMs, separated by vertical datum.

CUDEM Errors and Distributions (N = 10,136,126 cells)

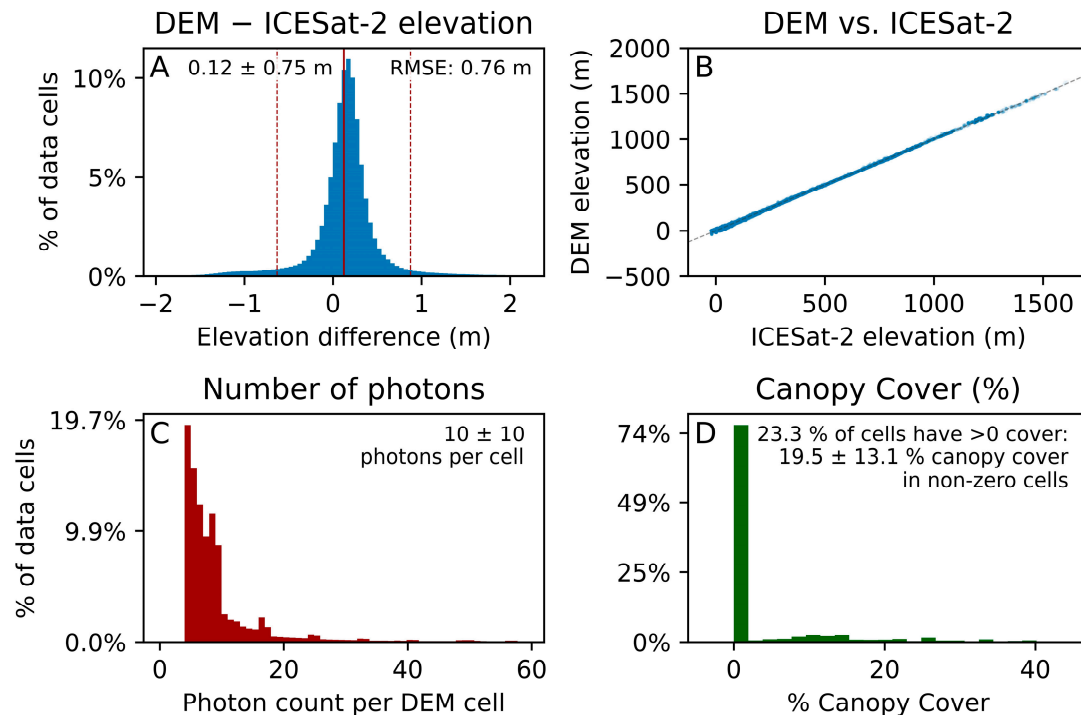


Figure 5. Independent validation results from ICESat-2 ground photons indicate a vertical mean bias error of $0.12 \text{ m} \pm 0.75 \text{ m}$ at one standard deviation, with an overall RMSE of 0.76 m, for the land portions of the 1/9th arc-second CUDEMs. (A) Histogram of DEM grid cell errors calculated as the differences with ICESat-2 derived elevations, including mean biases and standard deviations of errors. Note: Errors and biases result from both errors inherent in either DEMs or ICESat-2 and potential errors introduced by the vertical datum conversions. (B) DEM vs. ICESat-2 elevation scatterplot, with a dotted-gray “perfect fit” 1:1 line. (C) Histogram of the number of photons within the interdecile range that was used to compute the ICESat-2-derived mean elevation of each DEM grid cell. (D) Histogram of relative canopy-cover in the validated grid cells, with the percentage equated as the $(\# \text{ canopy photons}) / (\# \text{ canopy photons} + \# \text{ land photons}) \times 100$.

Table 7. Vertical accuracy statistics of CUDEMs calculated from ICESat-2, separated by vertical datum.

CUDEM Subset Location: Vertical Datum	Mean Error \pm One Standard Deviation (m)	Root Mean Square Error (RMSE) (m)
Entire CUDEM collection: Varies	0.12 ± 0.75	0.76
CONUS: NAVD88	0.12 ± 0.72	0.73
Hawaii: MSL	-0.45 ± 4.03	4.06
Puerto Rico: PRVD02	0.24 ± 1.15	1.18
USVI: VIVD09	0.78 ± 2.55	2.66
Guam: GUV04	-0.51 ± 1.20	1.30
CNMI: NMVD03	-0.54 ± 1.27	1.38
American Samoa: ASVD02	0.57 ± 2.78	2.84

4. Discussion

4.1. Benefits of CUDEM Program

NCEI CUDEMs are essential datasets for the coastal inundation modeling components of the NOAA Tsunami Program, NTHMP, COASTAL Act, and NOPP. The publicly available CUDEMs are also important datasets for numerous external coastal inundation modeling efforts. For example, CUDEMs were used to model susceptibility of barrier island road networks [83] and the evolution of barrier islands during extreme storms [84]. CUDEMs were also used to project the effects of land subsidence and sea-level rise on storm surge flooding [85], quantify tidal phase effects on coastal flooding [86], simulate compound coastal flooding [87], and to model coastal wetlands exposure to storm surge and waves [88]. A variety of other academic and federal agency coastal modeling research efforts use CUDEMs, e.g., coastal habitat monitoring [89,90], estimating estuarine stratification and flushing times [91], and modeling the impacts of dredging and sediment shoaling on hydrographic navigation [92,93]. CUDEMs are also important datasets for satellite-derived bathymetry [94], the generation of unstructured global ocean models [95], and as part of a USGS database of cross-shore profiles of U.S. Atlantic and Gulf of Mexico sandy coastlines [96].

The CUDEMs have been recognized for their use by multiple U.S. federal agencies towards meeting their shared mission goals. The Geospatial Data Act of 2018 (GDA) was signed into U.S. law on 5 October 2018, and is now in the U.S. Code, Title 43—Public Lands, Chapter 46: GEOSPATIAL DATA [97]. As part of the GDA, the FGDC was tasked to lead the development, implementation, and review of policies, practices, and standards relating to geospatial data, including the designation and oversight of National Geospatial Data Asset (NGDA) data themes. The CUDEMs are recognized as an official NGDA in the “elevation” data theme. Further, the NOAA Digital Coast DAV provides download statistics on all hosted datasets [98]. As of October 2022, CUDEMs have been downloaded over 9000 times, with a clear increase over time (Figure 6). The download counts are further classified by the email account domain extensions and indicate the use of the CUDEMs by the general public (.com; ~68%), academic researchers (.edu; ~17%), government officials (.gov; ~7%), and military entities (.mil; ~4%). The CUDEM dataset for the CONUS, “Continuously Updated Digital Elevation Model (CUDEM)—Ninth Arc-Second Resolution Bathymetric-Topographic Tiles,” has over 8000 downloads since 2018. These CUDEMs are the most downloaded DEM collection and 3rd most downloaded dataset hosted on the entire NOAA Digital Coast DAV since 2018.

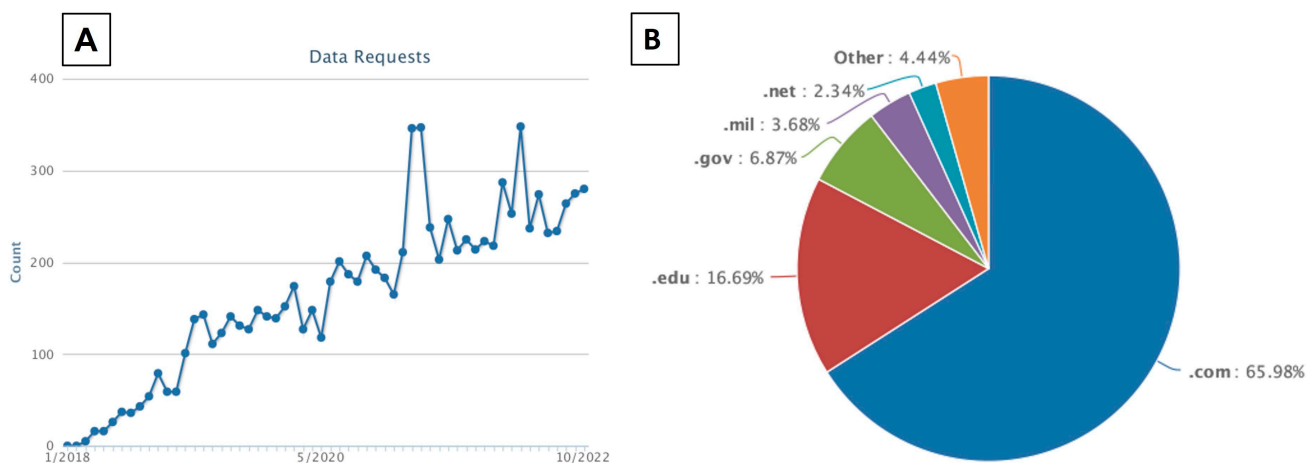


Figure 6. Download requests for CUDEMs from January 2018 to October 2022 by (A) total counts and (B) email domains. Download statistics and figures were generated from the NOAA Digital Coast Data Access Viewer—Data Report [98].

4.1.1. Rapid Update of CUDEMs

There are numerous benefits of a consistent, multi-resolution collection of continuously updated DEMs to NOAA, other federal science agencies, academic researchers, emergency management, and the general public. The CUDEM Program maximizes the value of the NOAA-funded data collections by rapidly incorporating these data into a quality-controlled, integrated topographic-bathymetric gridded data product. The CUDEM Program also benefits other U.S. governmental agencies that collect topographic and bathymetric data (e.g., USGS, FEMA, USACE) by similarly facilitating the rapid ingestion of these data collections into quality-controlled DEMs. The “waffles” module “stacks” can generate “version 2” CUDEMs with a raster stacking method where new data collections can be gridded, and then supersede areas of the “version 1” CUDEMs to rapidly update the DEM tile. Coastal process modelers often require a seamless, topographic-bathymetric DEM that is derived from numerous individual source datasets. Minimizing the time to incorporate the most recent topographic and bathymetric datasets into quality-controlled DEMs is imperative for accurate, present-day coastal process modeling. To date, we have updated 91 1/9th and 21 1/3rd DEM tiles in the CUDEM framework. Updated “version 2” DEMs include coastal areas with post-Hurricane Sandy data collections in New Jersey, post-Hurricane Harvey data collections in Texas, and post-Hurricane Maria data collections in Puerto Rico and USVI. These “version 2” DEMs are denoted in the naming convention as “_v2.tif.” We plan to continue to update CUDEM tiles with new data collections, eventually resulting in “version 3”, “version 4,” etc., DEMs.

4.1.2. Consistency across Spatial Scales

The Bipartisan Budget Act of 2018 funded research on new software tools to facilitate the rapid incorporation of updated local DEMs into regional and global elevation models. This research maximizes the value of post-storm data and ensures scientific modeling efforts utilize elevation models that best reflect the current morphology across spatial scales. The “waffles” module “stacks” can also be used to generate regional and global DEMs based on a raster stacking method where local, high-resolution 1/9th and 1/3rd arc-second CUDEM tiles supersede coarser regional and global datasets and thereby minimize DEM value discrepancies at the domain boundaries of local CUDEM tiles, regional CRMs, and the global ETOPO model. Such DEM value consistency is an important feature for modeling oceanic and coastal processes between nested spatial scales, such as tsunami propagation and inundation modeling, which require less than 1% difference between the ocean depth or elevation data found for the same location on two grids of differing resolutions to prevent model errors [99,100]. The multiscale DEM development framework was advanced through the Bipartisan Budget Act of 2018 with the rapid generation of post-Hurricane Harvey and Maria DEMs, a regional CRM of Puerto Rico and USVI, and post-Hurricane Irma DEMs planned for completion in 2023. Further, we recently generated a new, global relief model, ETOPO 2022, in the CUDEM framework that incorporated all the 1/9th and 1/3rd arc-second DEM tiles [72].

4.2. Challenges

There are many challenges to generating seamless, coastal DEMs when integrating disparate bathymetric and topographic data sources [14]. In most U.S. coastal areas, there are numerous high-accuracy, dense, modern topographic and topographic-bathymetric lidar datasets nearshore compared to low-accuracy, sparse, historical hydrographic soundings offshore. Determining the appropriate spatial resolution of the DEM is a fundamental question with raster-based DEMs with uniform cell sizes [101]. Amante [18] indicated that integrating disparate bathymetric and topographic datasets of varying age, quality, and measurement density results in areas of larger cell-level uncertainty within a CUDEM tile area. The terrain itself also varies within a DEM area, and, consequently, DEMs with a uniform resolution of 1/9th arc-second can have “hotspots” of larger cell-level uncertainty in areas of steeper terrain slope [18]. We generate integrated topographic-bathymetric CUD-

EMs at 1/9th arc-second and offshore bathymetric CUDEMs at 1/3rd arc-second resolution to best mimic typical topographic and bathymetric data densities and to meet coastal modeler requirements based on the resolutions of their nested structured grids or unstructured meshes. These grids and meshes used to model coastal inundation are typically 1 to 3 m in important nearshore hydrological channels and coarser than 10 m offshore.

Another major challenge is the lack of publicly available river and dredged channel bathymetry data. Huang et al. [102] indicated that “broken” bathymetric channels in coastal DEMs are a major source of over-attenuated tidal signals and water-level modeling errors. See Figures 17 and 18 in Huang et al. [102] for an example of improvements to the representation of bathymetric channels in recent CUDEMs and its impact on improving simulated water levels near Sabine Lake, Texas. Accurate river bathymetry representations are also important for modeling compound flooding that incorporates both storm surge and waves as well as freshwater inputs from tropical cyclones [61,95,103–107]. Flooding from Hurricane Harvey in Texas in 2017 exemplifies the need for accurate riverine flood modeling components to model compound flooding impacts of tropical cyclones [87,105,107,108]. Where areas lack river bathymetry data, interpolated values in DEMs across river channels can cause artificial dams due to adjacent topography or are inaccurately flattened at the bank elevation of channels. Future efforts should focus on discovering and incorporating additional locally funded sonar and lidar collections in dredged and inland river channels and performing additional research on optimally interpolated bathymetry in the absence of such data. Incorporating and enhancing previous research on optimally interpolating riverbed depths [109–113] that consider river anisotropy and that are hydrologically conditioned to flow downstream to the ocean is an area ripe for additional research in the CUDEM program.

Quantitative accuracy assessments of bathymetric DEMs remains an ongoing challenge and another area of prospective research for the CUDEM program. The current best-practice at NCEI is to QC bathymetric DEMs with visual methods including hillshades, 3-dimensional perspective images, and derived terrain slope and curvature rasters to identify and resolve data artifacts resulting from inaccurate hydrographic soundings and interpolation. We did not rigorously quantify the accuracy in bathymetry in the CUDEM tiles due to the lack of high-accuracy, independent measurements. Typically, we incorporated any high-quality bathymetric data into the CUDEMs, and, therefore, such data were not used as independent validation.

At this time, ICESat-2 returns were only used to validate CUDEM tiles over topographic land surfaces. The 532 nm green laser on the ICESat-2 ATLAS instrument can penetrate water, but the ATL03 product does not currently account for the refraction and the corresponding change in the speed of light that occurs at the air–water interface [114]. Parrish et al. [114] developed a refraction correction algorithm to measure seafloor returns at depths down to 40 m and calculated a corresponding RMSE of 0.43–0.60 m against high-accuracy airborne bathymetric lidar. However, ICESat-2 bathymetric returns are only available over limited regions with low turbidity and waves, and we did not use ICESat-2 to validate the bathymetry of CUDEM tiles. Bathymetric validation remains an area of future research interest and we may use ICESat-2 derived products for such validation as they are expanded and made available.

There are also limits to using ICESat-2 to assess the accuracy of the topography of the bare-earth CUDEMs at their native spatial resolution. Although ICESat-2 emits pulses at approximately 0.7 m intervals along-track, the footprint of each laser pulse is approximately 17 m in diameter [115], which is significantly larger than the ~3 m ground diameter of a CUDEM 1/9th arc-second grid cell. Latitude and longitude locations of individual ICESat-2 photons represent the center-location of a laser pulse, but the actual photon detected may come from anywhere within the ground footprint of the pulse. Thus, individual photons identified as ground or canopy may come from neighboring grid cells adjacent to the reported center-location of ICESat-2 returns. The greatest impacts from the larger laser pulse footprints would be in regions with steep terrain slope and/or large spatial heterogeneity

(e.g., a boulder field). The ICESat-2 photons also typically have a vertical uncertainty of approximately 10 cm [116], which contributes to the total error budget between ICESat-2 and the CUDEMs. Further, the ICESat-2 photon classification algorithm in NASA's ATL08 product differentiates between ground and canopy photons using a statistical surface-finding approach [79]. Although the algorithm performs well overall, independent assessments have found misidentified ground and canopy photons [117], which can bias the ICESat-2 ground elevation measurements. Lastly, building footprints in OpenStreetMap data can be incomplete over regions and subject to temporal changes between the time of CUDEM generation and ICESat-2 assessments, which may cause the extents of buildings to not be properly masked in certain locations. For these reasons, the calculated CUDEM vertical errors represent a combination of vertical errors in the DEM itself and potential errors in the ICESat-2 elevation product and building masking procedure. The respective contributions of each of these sources of error to the accuracy assessment of the CUDEM tiles are both terrain- and time-dependent and were not rigorously quantified in this analysis.

4.3. Future Work

We plan to continue to update NCEI DEM tiles in the CUDEM framework where new source data are available, especially in dynamic areas of morphologic change after hurricane or tsunami events. Our funding partners will inform the priority of specific regions for DEM updates to improve their respective modeling efforts. Areas of inland river bathymetry are the largest data gaps in the current collection of CUDEMs. A future research endeavor is to discover and incorporate additional local river bathymetry data collections and to perform research on optimizing riverbed interpolation to help improve the accuracy of storm surge and riverine compound flooding. We are also currently incorporating local DEM tiles into regional CRMs to enhance consistency in our elevation products. We plan to regularly update NCEI's suite of local, regional, and global DEMs to ensure seamless, gridded data products across spatial scales.

Future research will also focus on additional accuracy assessments with ICESat-2 passes, including new accuracy assessments of near-shore bathymetry where water turbidity and wave action permit. Previous research at NCEI indicates that the vertical uncertainty in DEMs varies spatially due to the integration of disparate data collected at different time periods with different measurement technologies (e.g., sonar, lidar), and for different terrain characteristics (e.g., sloped vs. flat terrain) [18,20]. DEM uncertainty affects the fidelity of coastal inundation modeling; therefore, the DEM uncertainty should be estimated and incorporated in such coastal process models [18,118–121]. Furthermore, identifying U.S. coastal communities and offshore waters with large DEM uncertainty also aids in prioritizing future topographic and bathymetric data collections, which, in turn, will also improve the fidelity of coastal inundation modeling.

We are also collaborating with the USGS on generating spatially explicit rasters that represent the total propagated vertical uncertainty at one standard deviation for each DEM cell. The total propagated vertical uncertainty could include uncertainty contributions from the data sources' measurement uncertainty from vendor reports, vertical datum transformation uncertainty provided by NOAA's VDatum tool [122], subcell measurement variance from the mean elevation of the DEM cell value, and the number of measurements per DEM cell, following the methodology from Amante (2018) [18] and references therein. This approach could also be informed by mapping potential biases in coastal marshes using remotely sensed coastal land cover products, such as NOAA's Coastal Change and Assessment Program (C-CAP) products, and tidal wetland biomass products [123,124]. New research on uncertainty contributions from morphologic change would also add to the utility of the DEMs for coastal modelers, especially in dynamic, sandy environments prone to erosion and accretion during storms and tsunamis.

Future research efforts to generate additional ancillary data products could enhance the scientific benefits of the CUDEM Program. We plan to generate new versions of the CUDEMs that will facilitate the analysis of morphologic change over time due to coastal

erosion and accretion on a tile-by-tile basis, especially pre- and post-storm or tsunami events. An example of pre- and post-Hurricane Michael DEMs of Cape San Blas, Florida, shown in Figure 7 highlights this avenue of future research efforts. Important derived data products could include morphologic change calculations representing the elevation differences between the pre- and post-event DEMs in areas with high-quality (i.e., lidar) datasets as indicated by the spatial metadata. Additional data products that indicate areas of new high-quality source data compared to previously interpolated elevations and depths can provide information on the return on investment for such data collections. Further, products representing areas of remaining elevation and depth data gaps can also aid in the prioritization of future data collections, which could then be incorporated in new versions of the CUDEMs.

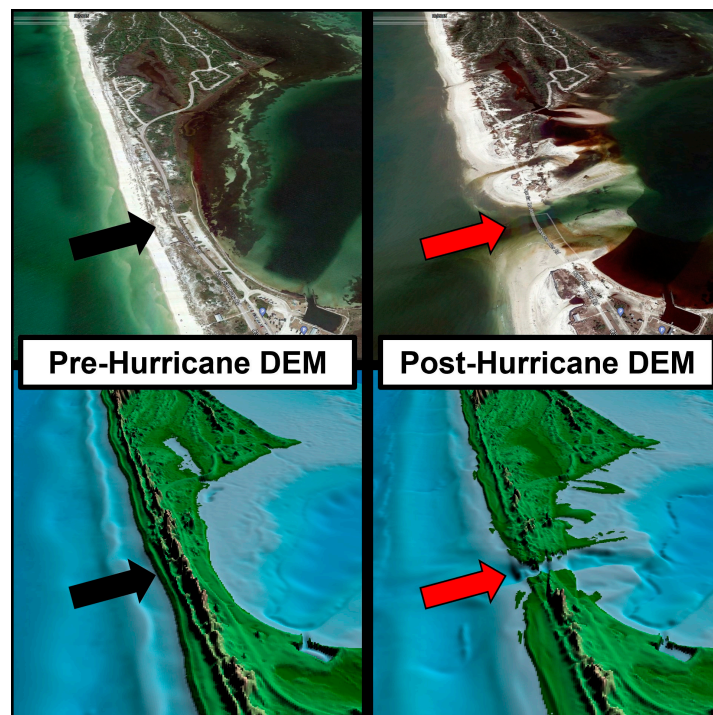


Figure 7. An example of pre- and post-Hurricane Michael DEMs of Cape San Blas, Florida. Quantifying morphologic change in CUDEMs from pre- and post-Hurricane DEMs, such as the Cape San Blas breach (arrows), is an avenue of future research.

5. Conclusions

We initiated a comprehensive program at NOAA NCEI, the CUDEM Program, to systematically develop DEMs using FOSS. We provide open-access to our code repository for consistency, transparency, and to promote accessibility. In this framework, we generated 1328 CUDEM tiles between 2014 and 2022, covering approximately 850,000 km² of U.S. coastal areas. To date, we have updated 112 of these CUDEM tiles with post-Hurricane Sandy, Harvey, and Maria topographic and bathymetric data collections. The CUDEMs are currently the highest-resolution, seamless depiction of the entire U.S. Atlantic and Gulf Coasts in the public domain. Further, the CUDEMs provide complete coverage for Hawaii and the U.S. island territories of Puerto Rico, USVI, American Samoa, Guam, and CNMI, and provide partial coverage for the U.S. Pacific Coast. Collectively, these DEMs are essential to determining the timing and extent of coastal inundation and improving community preparedness, event forecasting, and warning systems. We independently validated the land portions of the CUDEMs with NASA's ATLAS instrument on board the ICESat-2 observatory and calculated a corresponding vertical mean bias error of $0.12 \text{ m} \pm 0.75 \text{ m}$ at one standard deviation, with an overall RMSE of 0.76 m.

The CUDEMs were generated in a systematic framework to facilitate rapid updates and to enhance consistency across local, regional, and global scale DEMs. We plan to continue to generate new and updated DEMs in the CUDEM framework and perform additional accuracy assessments. Generated spatial metadata can help users infer the relative accuracy of areas within the DEM based on the age, density, and instrumentation of the underlying source data in the CUDEMs. Spatial metadata will also inform both future CUDEM updates and morphologic change analyses by delineating areas with high-quality pre- and post-event data collections. We plan to generate additional data products, such as spatially explicit vertical error estimations and morphologic change calculations, to enhance the utility and scientific benefits of the CUDEM Program.

Author Contributions: Conceptualization, C.J.A., M.L., K.C., M.G.S., M.M. and E.L.; methodology, C.J.A., M.L., K.C. and M.G.S.; data curation, C.J.A., M.L., K.C., M.G.S., M.M. and E.L.; validation, M.M. and M.L.; software, M.L., C.J.A. and M.M.; writing—original draft preparation, C.J.A.; writing—review and editing, C.J.A., M.L., K.C., M.G.S., M.M. and E.L. All authors have read and agreed to the published version of the manuscript.

Funding: This research was funded by NOAA cooperative agreement NA17OAR4320101 and NA19NES0220001, and by U.S. Geological Survey under Grant/Cooperative Agreement No. G22AC00053.

Data Availability Statement: The data presented in this study are available in Table 5 and by request from the corresponding author. The data development code is available at <https://github.com/ciresdem/cudem> (accessed on 14 March 2023).

Acknowledgments: We thank Kelly Stroker, Nicolás Arcos, and Barry Eakins for their leadership and support of the DEM Team at NOAA NCEI, and Matthew Stiller for the development of the American Samoa CUDEMs. We also thank the three anonymous reviewers for their valuable feedback that significantly improved the quality of the manuscript.

Conflicts of Interest: The authors declare no conflict of interest.

References

1. NOAA. What Percentage of the American Population Lives Near the Coast? Available online: <https://oceanservice.noaa.gov/facts/population.html> (accessed on 8 December 2022).
2. Amante, C.; Eakins, B. *ETOPO1 1 Arc-Minute Global Relief Model: Procedures, Data Sources and Analysis*; NOAA: Boulder, CO, USA, 2009. [CrossRef]
3. Amante, C.; Love, M.R.; Taylor, L.A.; Eakins, B.W. *Digital Elevation Models of Panama City, Florida: Procedures, Data Sources, and Analysis*; NOAA: Boulder, CO, USA, 2011.
4. Love, M.R.; Amante, C.; Taylor, L.A.; Eakins, B.W. *Digital Elevation Models of New Orleans, Louisiana: Procedures, Data Sources, and Analysis*; NOAA: Boulder, CO, USA, 2011.
5. Amante, C.; Love, M.R.; Taylor, L.A.; Eakins, B.W. *Digital Elevation Models of Mobile, Alabama: Procedures, Data Sources, and Analysis*; NOAA: Boulder, CO, USA, 2011.
6. Carignan, K.S.; Taylor, L.A.; Eakins, B.W.; Caldwell, R.J.; Friday, D.Z.; Grothe, P.R.; Lim, E. *Digital Elevation Models of Central California and San Francisco Bay: Procedures, Data Sources, and Analysis*; NOAA: Boulder, CO, USA, 2011.
7. Lim, E.; Taylor, L.A.; Eakins, B.W.; Carignan, K.S.; Warnken, R.R.; Medley, P.R. *Digital Elevation Models of Craig, Alaska: Procedures, Data Sources and Analysis*; NOAA: Boulder, CO, USA, 2009.
8. Lim, E.; Taylor, L.A.; Eakins, B.W.; Carignan, K.S.; Warnken, R.R.; Medley, P.R. *Digital Elevation Model of Portland, Maine: Procedures, Data Sources and Analysis*; NOAA: Boulder, CO, USA, 2009.
9. Caldwell, R.J.; Taylor, L.A.; Eakins, B.W.; Carignan, K.S.; Grothe, P.R.; Lim, E.; Friday, D.Z. *Digital Elevation Models of Santa Monica, California: Procedures, Data Sources, and Analysis*; NOAA: Boulder, CO, USA, 2011.
10. Grothe, P.R.; Taylor, L.A.; Eakins, B.W.; Carignan, K.S.; Caldwell, R.J.; Lim, E.; Friday, D.Z. *Digital Elevation Models of the Virgin Islands: Procedures, Data Sources and Analysis*; NOAA: Boulder, CO, USA, 2012.
11. Friday, D.Z.; Taylor, L.A.; Eakins, B.W.; Warnken, R.R.; Carignan, K.S.; Caldwell, R.J.; Lim, E.; Grothe, P.R. *Digital Elevation Models of Palm Beach, Florida: Procedures, Data Sources and Analysis*; NOAA: Boulder, CO, USA, 2012.
12. NOAA National Geophysical Data Center. *U.S. Coastal Relief Model Vol.1—Northeast Atlantic 1999*; NOAA: Washington, DC, USA, 1999. [CrossRef]
13. Danielson, J.J.; Poppenga, S.K.; Brock, J.C.; Evans, G.A.; Tyler, D.J.; Gesch, D.B.; Thatcher, C.A.; Barras, J.A. Topobathymetric Elevation Model Development using a New Methodology: Coastal National Elevation Database. *J. Coast. Res.* **2016**, *76*, 75–89. [CrossRef]
14. Eakins, B.W.; Grothe, P.R. Challenges in Building Coastal Digital Elevation Models. *J. Coast. Res.* **2014**, *30*, 942–953. [CrossRef]

15. Gesch, D.; Wilson, R. Development of a Seamless Multisource Topographic/Bathymetric Elevation Model of Tampa Bay. *Mar. Technol. Soc. J.* **2001**, *35*, 58–64. [[CrossRef](#)]
16. Thatcher, C.A.; Brock, J.C.; Danielson, J.J.; Poppenga, S.K.; Gesch, D.B.; Palaseanu-Lovejoy, M.E.; Barras, J.A.; Evans, G.A.; Gibbs, A.E. Creating a Coastal National Elevation Database (CoNED) for Science and Conservation Applications. *J. Coast. Res.* **2016**, *76*, 64–74. [[CrossRef](#)]
17. Amante, C. Consideration of Elevation Uncertainty in Coastal Flood Models. 2018. Available online: https://scholar.colorado.edu/concern/graduate_thesis_or_dissertations/fq977t92p (accessed on 14 March 2023).
18. Amante, C.J. Estimating Coastal Digital Elevation Model Uncertainty. *J. Coast. Res.* **2018**, *34*, 1382–1397. [[CrossRef](#)]
19. Hare, R.; Eakins, B.; Amante, C. Modelling bathymetric uncertainty. *Int. Hydrogr. Rev.* **2011**, *6*, 31–42.
20. Amante, C.J.; Eakins, B.W. Accuracy of Interpolated Bathymetry in Digital Elevation Models. *J. Coast. Res.* **2016**, *76*, 123–133. [[CrossRef](#)]
21. Taylor, L.A.; Eakins, B.W. Seamlessly integrating bathymetric and topographic data to support tsunami modeling and forecasting efforts. In *Ocean Globe*; Breman, J., Ed.; ESRI Press Academic: Redlands, CA, USA, 2010; pp. 37–56, ISBN 978-1-58948-219-7.
22. Hébert, H.; Heinrich, P.; Schindelé, F.; Piatanesi, A. Far-field simulation of tsunami propagation in the Pacific Ocean: Impact on the Marquesas Islands (French Polynesia). *J. Geophys. Res. Ocean.* **2001**, *106*, 9161–9177. [[CrossRef](#)]
23. Kowalik, Z.; Knight, W.; Logan, T.; Whitmore, P. Numerical modeling of the global tsunami: Indonesian Tsunami of 26 December 2004. *Sci. Tsunami Hazards* **2004**, *23*, 40–56.
24. Kowalik, Z.; Horrillo, J.; Knight, W.; Logan, T. Kuril Islands tsunami of November 2006: 1. Impact at Crescent City by distant scattering. *J. Geophys. Res. Ocean.* **2008**, *113*, 1–11. [[CrossRef](#)]
25. Horrillo, J.; Knight, W.; Kowalik, Z. Kuril Islands tsunami of November 2006: 2. Impact at Crescent City by local enhancement. *J. Geophys. Res. Ocean.* **2008**, *113*, 1–12. [[CrossRef](#)]
26. Titov, V.; Rabinovich, A.B.; Mofjeld, H.O.; Thomson, R.E.; González, F.I. The Global Reach of the 26 December 2004 Sumatra Tsunami. *Science* **2005**, *309*, 2045–2048. [[CrossRef](#)] [[PubMed](#)]
27. Beck, M.W.; Losada, I.J.; Menéndez, P.; Reguero, B.G.; Díaz-Simal, P.; Fernández, F. The global flood protection savings provided by coral reefs. *Nat. Commun.* **2018**, *9*, 2186. [[CrossRef](#)]
28. Rey, W.; Mendoza, E.T.; Salles, P.; Zhang, K.; Teng, Y.-C.; Trejo-Rangel, M.A.; Franklin, G.L. Hurricane flood risk assessment for the Yucatan and Campeche State coastal area. *Nat. Hazards* **2019**, *96*, 1041–1065. [[CrossRef](#)]
29. Hopkins, J.; Elgar, S.; Raubenheimer, B. Observations and model simulations of wave-current interaction on the inner shelf. *J. Geophys. Res. Ocean.* **2016**, *121*, 198–208. [[CrossRef](#)]
30. Hopkins, J.; Elgar, S.; Raubenheimer, B. Storm Impact on Morphological Evolution of a Sandy Inlet. *J. Geophys. Res. Ocean.* **2018**, *123*, 5751–5762. [[CrossRef](#)]
31. NOAA National Geophysical Data Center. *5-Minute Gridded Global Relief Data (ETOPO5)*; NOAA: Boulder, CO, USA, 1993. [[CrossRef](#)]
32. NOAA National Geophysical Data Center. *2-Minute Gridded Global Relief Data (ETOPO2) Version 2*; NOAA: Boulder, CO, USA, 2006. [[CrossRef](#)]
33. NOAA National Geophysical Data Center. *U.S. Coastal Relief Model Vol. 2—Southeast Atlantic*; NOAA: Boulder, CO, USA, 1999. [[CrossRef](#)]
34. NOAA National Geophysical Data Center. *U.S. Coastal Relief Model Vol. 3—Florida and East Gulf of Mexico*; NOAA: Boulder, CO, USA, 2001.
35. NOAA National Geophysical Data Center. *U.S. Coastal Relief Model Vol. 4—Central Gulf of Mexico*; NOAA: Boulder, CO, USA, 2001.
36. NOAA National Geophysical Data Center. *U.S. Coastal Relief Model Vol. 5—Western Gulf of Mexico*; NOAA: Boulder, CO, USA, 2001. [[CrossRef](#)]
37. NOAA National Geophysical Data Center. *U.S. Coastal Relief Model Vol. 6—Southern California*; NOAA: Boulder, CO, USA, 2003. [[CrossRef](#)]
38. NOAA National Geophysical Data Center. *U.S. Coastal Relief Model Vol. 7—Central Pacific*; NOAA: Boulder, CO, USA, 2003. [[CrossRef](#)]
39. NOAA National Geophysical Data Center. *U.S. Coastal Relief Model Vol. 8—Northwest Pacific*; NOAA: Boulder, CO, USA, 2003. [[CrossRef](#)]
40. NOAA National Geophysical Data Center. *U.S. Coastal Relief Model Vol. 9—Puerto Rico*; NOAA: Boulder, CO, USA, 2005. [[CrossRef](#)]
41. NOAA National Geophysical Data Center. *U.S. Coastal Relief Model—Southern California Version 2*; NOAA: Boulder, CO, USA, 2012. [[CrossRef](#)]
42. NOAA National Geophysical Data Center. *Southern Alaska Coastal Relief Model*; NOAA: Boulder, CO, USA, 2009. [[CrossRef](#)]
43. Taylor, L.A.; Eakins, B.W.; Warnken, R.R.; Carignan, K.S.; Sharman, G.F.; Schoolcraft, D.C.; Sloss, P.W. *Digital Elevation Models of Myrtle Beach, South Carolina: Procedures, Data Sources and Analysis*; NOAA: Boulder, CO, USA, 2008.
44. Taylor, L.A.; Eakins, B.W.; Carignan, K.S.; Warnken, R.R.; Sazonova, T.S.; Schoolcraft, D.C. *Digital Elevation Model of Galveston, Texas: Procedures, Data Sources and Analysis*; NOAA: Boulder, CO, USA, 2008.

45. Eakins, B.W.; Taylor, L.A.; Carignan, K.S.; Warnken, R.R.; Lim, E.; Medley, P.R. *Digital Elevation Model of Nantucket, Massachusetts: Procedures, Data Sources and Analysis*; NOAA: Boulder, CO, USA, 2009.
46. Eakins, B.; Danielson, J.J.; Sutherland, M.; Mclean, S. A framework for a seamless depiction of merged bathymetry and topography along US coasts. In Proceedings of the US HYDRO Conference Proceedings, National Harbor, MD, USA, 16–19 March 2015.
47. Gica, E. *A Tsunami Forecast Model for Kihei, Hawaii*; NOAA: Seattle, WA, USA, 2015. [CrossRef]
48. Gica, E. *A Tsunami Forecast Model for Midway Atoll*; NOAA: Seattle, WA, USA, 2015. [CrossRef]
49. Gica, E. *A Tsunami Forecast Model for Santa Barbara, California*; NOAA: Seattle, WA, USA, 2015. [CrossRef]
50. Titov, V.V.; Gonzalez, F.I.; Bernard, E.N.; Eble, M.C.; Mofjeld, H.O.; Newman, J.C.; Venturato, A.J. Real-Time Tsunami Forecasting: Challenges and Solutions. *Nat. Hazards* **2005**, *35*, 35–41. [CrossRef]
51. Adams, L.M.; Gonzalez, F.I.; LeVeque, R.J. Tsunami Hazard Assessment of Whatcom County, Washington, Project Report—Version 2. 2019. Available online: <https://digital.lib.washington.edu/researchworks/handle/1773/45586> (accessed on 14 March 2023).
52. LeVeque, R.J.; Gonzalez, F.I.; Adams, L.M. Tsunami Hazard Assessment of Snohomish County, Washington. 2021. Available online: http://depts.washington.edu/ptha/WA_EMD_Snoho2/SnohomishCountyTHAv3_2021-02-05.pdf (accessed on 14 March 2023).
53. LeVeque, R.J.; Adams, L.M.; Gonzalez, F.I. Tsunami Hazard Assessment of Northwestern Coast of Washington. 2021. Available online: http://depts.washington.edu/ptha/WA_EMD_2020/NWWA_THA.pdf (accessed on 14 March 2023).
54. Titov, V.V.; Arcas, D.; Moore, C.W.; LeVeque, R.J.; Adams, L.M.; Gonzalez, F.I. Tsunami Hazard Assessment of Bainbridge Island, Washington. 2018. Available online: http://depts.washington.edu/ptha/WA_EMD_Bainbridge/BainbridgeIslandTHA_draft2_0181130b.pdf (accessed on 14 March 2023).
55. Arcas, D.; Gica, E.; Titov, V.V. *Tsunami Inundation Modeling of San Juan Islands, Washington, Due to a Cascadia Subduction Zone Earthquake*; NOAA: Seattle, WA, USA, 2020. [CrossRef]
56. Allan, J.; Zhang, J.; O'Brien, F. Open-File Report O-21-08, Tsunami Inundation Modeling Update for the Northern Oregon Coast: Tillamook and Clatsop Counties. 2021. Available online: https://www.oregongeology.org/pubs/ofr/O-21-08_report.pdf (accessed on 14 March 2023).
57. Dolcimascolo, A.; Eungard, D.W.; Allen, C.; LeVeque, R.J.; Adams, L.M.; Arcas, D.; Titov, V.V.; González, F.I.; Moore, C.; Garrison-Laney, C.E.; et al. Tsunami Hazard Maps of the Puget Sound and Adjacent Waters—Model Results from an Extended L1 Mw 9.0 Cascadia Subduction Zone Megathrust Earthquake Scenario: Washington Geological Survey Map Series 2021-01. Available online: https://fortress.wa.gov/dnr/geologydata/tsunami_hazard_maps/ger_ms2021-01_tsunami_hazard_puget_sound.zip (accessed on 14 March 2023).
58. California Geological Survey. California Governor's Office of Emergency Services Tsunami Hazard Area Map, Humboldt County 2021. 2021. Available online: <https://www.conservation.ca.gov/cgs/tsunami/maps/humboldt> (accessed on 14 March 2023).
59. *Consumer Option for an Alternative System to Allocate Losses Act of 2012*; Public Law 112–141; U.S. Government Publishing Office: Washington, DC, USA, 2012. Available online: <https://www.govinfo.gov/content/pkg/PLAW-112publ141/pdf/PLAW-112publ141.pdf> (accessed on 14 March 2023).
60. Moghimi, S.; Van der Westhuysen, A.; Abdolali, A.; Myers, E.; Vinogradov, S.; Ma, Z.; Liu, F.; Mehra, A.; Kurkowski, N. Development of an ESMF Based Flexible Coupling Application of ADCIRC and WAVEWATCH III for High Fidelity Coastal Inundation Studies. *J. Mar. Sci. Eng.* **2020**, *8*, 308. [CrossRef]
61. van der Westhuysen, A.; Ogden, F.; Flowers, T.; Fanara, T.; Myers, E.; Dean, C.; Allen, A.; Lindley, C.; Zachry, B.; Fujisaki-Manome, A.; et al. *Whitepaper on the Development of a Unified Forecast System for Coastal Total Water Level Prediction*; NOAA: Silver Spring, MD, USA, 2022. [CrossRef]
62. *Bipartisan Budget Act of 2018*; Public Law 115–123; U.S. Government Publishing Office: Washington, DC, USA, 2018. Available online: <https://www.govinfo.gov/content/pkg/PLAW-115publ123/pdf/PLAW-115publ123.pdf> (accessed on 14 March 2023).
63. Goetz, J.; Brenning, A.; Marcer, M.; Bodin, X. Modeling the precision of structure-from-motion multi-view stereo digital elevation models from repeated close-range aerial surveys. *Remote Sens. Environ.* **2018**, *210*, 208–216. [CrossRef]
64. Hashemi-Beni, L.; Jones, J.; Thompson, G.; Johnson, C.; Gebrehiwot, A. Challenges and Opportunities for UAV-Based Digital Elevation Model Generation for Flood-Risk Management: A Case of Princeville, North Carolina. *Sensors* **2018**, *18*, 3843. [CrossRef] [PubMed]
65. Thomas, N.; Pertiwi, A.P.; Traganos, D.; Lagomasino, D.; Poursanidis, D.; Moreno, S.; Fatoyinbo, L. Space-Borne Cloud-Native Satellite-Derived Bathymetry (SDB) Models Using ICESat-2 And Sentinel-2. *Geophys. Res. Lett.* **2021**, *48*, e2020GL092170. [CrossRef]
66. Tanaka, H.; Adityawan, M.B.; Mano, A. Morphological changes at the Nanakita River mouth after the Great East Japan Tsunami of 2011. *Coast. Eng.* **2014**, *86*, 14–26. [CrossRef]
67. Haerens, P.; Bolle, A.; Trouw, K.; Houthuys, R. Definition of storm thresholds for significant morphological change of the sandy beaches along the Belgian coastline. *Geomorphology* **2012**, *143–144*, 104–117. [CrossRef]
68. Voudoukas, M.I.; Ranasinghe, R.; Mentaschi, L.; Plomaritis, T.A.; Athanasiou, P.; Luijendijk, A.; Feyen, L. Sandy coastlines under threat of erosion. *Nat. Clim. Chang.* **2020**, *10*, 260–263. [CrossRef]
69. Zachry, B.C.; Booth, W.J.; Rhome, J.R.; Sharon, T.M. A National View of Storm Surge Risk and Inundation. *Weather Clim. Soc.* **2015**, *7*, 109–117. [CrossRef]

70. Guth, P.L.; Van Niekerk, A.; Grohmann, C.H.; Muller, J.-P.; Hawker, L.; Florinsky, I.V.; Gesch, D.; Reuter, H.I.; Herrera-Cruz, V.; Riazanoff, S.; et al. Digital Elevation Models: Terminology and Definitions. *Remote Sens.* **2021**, *13*, 3581. [CrossRef]
71. Cooper, H.M.; Chen, Q.; Fletcher, C.H.; Barbee, M.M. Assessing vulnerability due to sea-level rise in Maui, Hawai'i using LiDAR remote sensing and GIS. *Clim. Chang.* **2013**, *116*, 547–563. [CrossRef]
72. NOAA National Centers for Environmental Information. *ETOPO 2022 15 Arc-Second Global Relief Model*; NOAA: Boulder, CO, USA, 2022. [CrossRef]
73. Love, M.; Amante, C.; Carignan, K.; MacFerrin, M.; Lim, E. CUDEM (Version 1.9.0) [Computer Software]. Available online: <https://github.com/ciresdem/cudem> (accessed on 8 December 2022).
74. Caress, D.; Chayes, D. MB-System (Version 5.7.8) [Computer Software]. Available online: <https://github.com/dwcaress/MB-System> (accessed on 8 December 2022).
75. Parker, B. The Integration of Bathymetry, Topography and Shoreline and the Vertical Datum Transformations behind It. *Int. Hydrogr. Rev.* **2002**, *3*, 14–26.
76. European Space Agency, Sinergise. *Copernicus Global Digital Elevation Model*, Distributed by OpenTopography. 2021. [CrossRef]
77. Virtanen, P.; Gommers, R.; Oliphant, T.E.; Haberland, M.; Reddy, T.; Cournapeau, D.; Burovski, E.; Peterson, P.; Weckesser, W.; Bright, J.; et al. SciPy 1.0: Fundamental algorithms for scientific computing in Python. *Nat. Methods* **2020**, *17*, 261–272. [CrossRef]
78. Neumann, T.A.; Brenner, A.; Hancock, D.; Robbins, J.; Saba, B.; Harbeck, K.; Gibbons, A.; Lee, J.; Luhcke, S.B.; Rebold, T. *ATLAS/ICESat-2 L2A Global Geolocated Photon Data, Version 5 [Data Set]*; NASA National Snow and Ice Data Center Distributed Active Archive Center: Boulder, CO, USA, 2021. [CrossRef]
79. Neuenschwander, A.L.; Pitts, K.L.; Jelley, B.P.; Robbins, J.; Klotz, B.; Popescu, C.; Nelson, R.F.; Harding, D.; Pederson, D.; Sheridan, R. *ATLAS/ICESat-2 L3A Land and Vegetation Height, Version 5 [Data Set]*; NASA National Snow and Ice Data Center Distributed Active Archive Center: Boulder, CO, USA, 2021. [CrossRef]
80. Messenger, M.L.; Lehner, B.; Grill, G.; Nedeva, I.; Schmitt, O. Estimating the volume and age of water stored in global lakes using a geo-statistical approach. *Nat. Commun.* **2016**, *7*, 13603. [CrossRef]
81. Haklay, M.; Weber, P. OpenStreetMap: User-Generated Street Maps. *IEEE Pervasive Comput.* **2008**, *7*, 12–18. [CrossRef]
82. NOAA. NOAA NCEI. Available online: https://www.ngdc.noaa.gov/mgg/dat/dems/tiled_tr/ (accessed on 1 November 2022).
83. Aldabet, S.; Goldstein, E.B.; Lazarus, E.D. Thresholds in Road Network Functioning on US Atlantic and Gulf Barrier Islands. *Earths Future* **2022**, *10*, e2021EF002581. [CrossRef]
84. Beckman, J.N.; Long, J.W.; Hawkes, A.D.; Leonard, L.A.; Ghoneim, E. Investigating Controls on Barrier Island Overwash and Evolution during Extreme Storms. *Water* **2021**, *13*, 2829. [CrossRef]
85. Johnston, J.; Cassalho, F.; Miesse, T.; Ferreira, C.M. Projecting the effects of land subsidence and sea level rise on storm surge flooding in Coastal North Carolina. *Sci. Rep.* **2021**, *11*, 21679. [CrossRef]
86. Marsooli, R.; Wang, Y. Quantifying Tidal Phase Effects on Coastal Flooding Induced by Hurricane Sandy in Manhattan, New York Using a Micro-Scale Hydrodynamic Model. *Front. Built Environ.* **2020**, *6*, 149. [CrossRef]
87. Stephens, T.A.; Savant, G.; Sanborn, S.C.; Wallen, C.M.; Roy, S. Monolithic Multiphysics Simulation of Compound Flooding. *J. Hydraul. Eng.* **2022**, *148*, 05022003. [CrossRef]
88. Cassalho, F.; Miesse, T.W.; de Lima, A.d.S.; Khalid, A.; Ferreira, C.M.; Sutton-Grier, A.E. Coastal Wetlands Exposure to Storm Surge and Waves in the Albemarle-Pamlico Estuarine System during Extreme Events. *Wetlands* **2021**, *41*, 49. [CrossRef]
89. Warnell, K.; Olander, L.; Currin, C. Sea level rise drives carbon and habitat loss in the U.S. mid-Atlantic coastal zone. *PLoS Clim.* **2022**, *1*, e0000044. [CrossRef]
90. Martinez, M.T.; Calle, L.; Románach, S.S.; Gawlik, D.E. Evaluating temporal and spatial transferability of a tidal inundation model for foraging waterbirds. *Ecosphere* **2022**, *13*, e4030. [CrossRef]
91. Shen, X.; Detenbeck, N.; You, M. Spatial and temporal variations of estuarine stratification and flushing time across the continental U.S. *Estuar. Coast. Shelf Sci.* **2022**, *279*, 108147. [CrossRef]
92. Lemke, L.; Janssen, M.S.; Miller, J.K. Mitigation of Channel Shoaling at a Sheltered Inlet Subject to Flood Gate Operations. *J. Mar. Sci. Eng.* **2020**, *8*, 865. [CrossRef]
93. Janssen, M.S.; Lemke, L.; Miller, J.K.; Douglas, W.S. Fortescue Inlet: Offshore Deposition Basins for Navigation Channel Management in Small Craft Inlets. *J. Waterw. Port Coast. Ocean Eng.* **2022**, *148*, 05021019. [CrossRef]
94. Ilori, C.O.; Knudby, A. An Approach to Minimize Atmospheric Correction Error and Improve Physics-Based Satellite-Derived Bathymetry in a Coastal Environment. *Remote Sens.* **2020**, *12*, 2752. [CrossRef]
95. Zhang, Y.J.; Fernandez-MontBlanc, T.; Pringle, W.; Yu, H.-C.; Cui, L.; Moghimi, S. Global seamless tidal simulation using a 3D unstructured-grid model. *Geosci. Model Dev. Discuss.* **2022**, 1–25. [CrossRef]
96. Mickey, R.C.; Passeri, D.L. A Database of Topo-Bathy Cross-Shore Profiles and Characteristics for U.S. Atlantic and Gulf of Mexico Sandy Coastlines. *Data* **2022**, *7*, 92. [CrossRef]
97. *FAA Reauthorization Act of 2018*; Public Law 115–254; U.S. Government Publishing Office: Washington, DC, USA, 2018. Available online: <https://www.govinfo.gov/content/pkg/PLAW-115publ254/pdf/PLAW-115publ254.pdf> (accessed on 14 March 2023).
98. NOAA. Digital Coast Data Access Viewer—Data Report. Available online: https://coast.noaa.gov/dataviewer_stats/ (accessed on 1 November 2022).
99. National Oceanic & Atmospheric Administration. *Method of Splitting Tsunami (MOST) Software Manual*; NOAA: Seattle, WA, USA, 2006.
100. Titov, V.V.; Gonzalez, F.I. *Implementation and Testing of the Method of Splitting Tsunami (MOST) Model*; NOAA: Seattle, WA, USA, 1997.

101. Hengl, T. Finding the right pixel size. *Comput. Geosci.* **2006**, *32*, 1283–1298. [\[CrossRef\]](#)
102. Huang, W.; Zhang, Y.J.; Wang, Z.; Ye, F.; Moghimi, S.; Myers, E.; Yu, H. Tidal simulation revisited. *Ocean Dyn.* **2022**, *72*, 187–205. [\[CrossRef\]](#)
103. Couasnon, A.; Eilander, D.; Muis, S.; Veldkamp, T.I.E.; Haigh, I.D.; Wahl, T.; Winsemius, H.C.; Ward, P.J. Measuring compound flood potential from river discharge and storm surge extremes at the global scale. *Nat. Hazards Earth Syst. Sci.* **2020**, *20*, 489–504. [\[CrossRef\]](#)
104. Zhang, Y.J.; Ye, F.; Yu, H.; Sun, W.; Moghimi, S.; Myers, E.; Nunez, K.; Zhang, R.; Wang, H.; Roland, A.; et al. Simulating compound flooding events in a hurricane. *Ocean Dyn.* **2020**, *70*, 621–640. [\[CrossRef\]](#)
105. Huang, W.; Ye, F.; Zhang, Y.J.; Park, K.; Du, J.; Moghimi, S.; Myers, E.; Pe'eri, S.; Calzada, J.R.; Yu, H.C.; et al. Compounding factors for extreme flooding around Galveston Bay during Hurricane Harvey. *Ocean Model.* **2021**, *158*, 101735. [\[CrossRef\]](#)
106. Kim, H.; Villarini, G.; Jane, R.; Wahl, T.; Misra, S.; Michalek, A. On the generation of high-resolution probabilistic design events capturing the joint occurrence of rainfall and storm surge in coastal basins. *Int. J. Climatol.* **2022**, *43*, 761–771. [\[CrossRef\]](#)
107. Loveland, M.; Kiaghadi, A.; Dawson, C.N.; Rifai, H.S.; Misra, S.; Mosser, H.; Parola, A. Developing a Modeling Framework to Simulate Compound Flooding: When Storm Surge Interacts With Riverine Flow. *Front. Clim.* **2021**, *2*, 609610. [\[CrossRef\]](#)
108. Valle-Levinson, A.; Olabarrieta, M.; Heilman, L. Compound flooding in Houston-Galveston Bay during Hurricane Harvey. *Sci. Total Environ.* **2020**, *747*, 141272. [\[CrossRef\]](#) [\[PubMed\]](#)
109. Merwade, V.; Cook, A.; Coonrod, J. GIS techniques for creating river terrain models for hydrodynamic modeling and flood inundation mapping. *Environ. Model. Softw.* **2008**, *23*, 1300–1311. [\[CrossRef\]](#)
110. Song, Y.; Huang, J.; Toorman, E.; Yang, G. Reconstruction of River Topography for 3D Hydrodynamic Modelling Using Surveyed Cross-Sections: An Improved Algorithm. *Water* **2020**, *12*, 3539. [\[CrossRef\]](#)
111. Merwade, V.M.; Maidment, D.R.; Goff, J.A. Anisotropic considerations while interpolating river channel bathymetry. *J. Hydrol.* **2006**, *331*, 731–741. [\[CrossRef\]](#)
112. Dysarz, T. Development of RiverBox—An ArcGIS Toolbox for River Bathymetry Reconstruction. *Water* **2018**, *10*, 1266. [\[CrossRef\]](#)
113. Caviedes-Voullième, D.; Morales-Hernández, M.; López-Marijuan, I.; García-Navarro, P. Reconstruction of 2D river beds by appropriate interpolation of 1D cross-sectional information for flood simulation. *Environ. Model. Softw.* **2014**, *61*, 206–228. [\[CrossRef\]](#)
114. Parrish, C.E.; Magruder, L.A.; Neuenschwander, A.L.; Forfinski-Sarkozi, N.; Alonzo, M.; Jasinski, M. Validation of ICESat-2 ATLAS Bathymetry and Analysis of ATLAS's Bathymetric Mapping Performance. *Remote Sens.* **2019**, *11*, 1634. [\[CrossRef\]](#)
115. Markus, T.; Neumann, T.; Martino, A.; Abdalati, W.; Brunt, K.; Csatho, B.; Farrell, S.; Fricker, H.; Gardner, A.; Harding, D.; et al. The Ice, Cloud, and land Elevation Satellite-2 (ICESat-2): Science requirements, concept, and implementation. *Remote Sens. Environ.* **2017**, *190*, 260–273. [\[CrossRef\]](#)
116. Magruder, L.; Neumann, T.; Kurtz, N. ICESat-2 Early Mission Synopsis and Observatory Performance. *Earth Space Sci.* **2021**, *8*, e2020EA001555. [\[CrossRef\]](#)
117. Tian, X.; Shan, J. Comprehensive Evaluation of the ICESat-2 ATL08 Terrain Product. *IEEE Trans. Geosci. Remote Sens.* **2021**, *59*, 8195–8209. [\[CrossRef\]](#)
118. Gesch, D.B. Consideration of Vertical Uncertainty in Elevation-Based Sea-Level Rise Assessments: Mobile Bay, Alabama Case Study. *J. Coast. Res.* **2013**, *63*, 197–210. [\[CrossRef\]](#)
119. Gesch, D.B. Best Practices for Elevation-Based Assessments of Sea-Level Rise and Coastal Flooding Exposure. *Front. Earth Sci.* **2018**, *6*, 230. [\[CrossRef\]](#)
120. Enwright, N.M.; Wang, L.; Borchert, S.M.; Day, R.H.; Feher, L.C.; Osland, M.J. The Impact of Lidar Elevation Uncertainty on Mapping Intertidal Habitats on Barrier Islands. *Remote Sens.* **2018**, *10*, 5. [\[CrossRef\]](#)
121. Amante, C.J. Uncertain seas: Probabilistic modeling of future coastal flood zones. *Int. J. Geogr. Inf. Sci.* **2019**, *33*, 2188–2217. [\[CrossRef\]](#)
122. NOAA. Estimation of Vertical Uncertainties in VDatum. Available online: https://vdatum.noaa.gov/docs/est_uncertainties.html (accessed on 7 March 2023).
123. Byrd, K.B.; Ballanti, L.; Thomas, N.; Nguyen, D.; Holmquist, J.R.; Simard, M.; Windham-Myers, L. A remote sensing-based model of tidal marsh aboveground carbon stocks for the conterminous United States. *ISPRS J. Photogramm. Remote Sens.* **2018**, *139*, 255–271. [\[CrossRef\]](#)
124. Byrd, K.B.; Ballanti, L.; Thomas, N.; Nguyen, D.; Holmquist, J.R.; Simard, M.; Windham-Myers, L. Corrigendum to “A remote sensing-based model of tidal marsh aboveground carbon stocks for the conterminous United States” [ISPRS J. Photogram. Rem. Sens. 139 (2018) 255–271]. *ISPRS J. Photogramm. Remote Sens.* **2020**, *166*, 63–67. [\[CrossRef\]](#)

Disclaimer/Publisher's Note: The statements, opinions and data contained in all publications are solely those of the individual author(s) and contributor(s) and not of MDPI and/or the editor(s). MDPI and/or the editor(s) disclaim responsibility for any injury to people or property resulting from any ideas, methods, instructions or products referred to in the content.